https://doi.org/10.1016/j.tws.2019.05.011

Mechanical properties of thin sheet steel after exposure to high temperatures

Yancheng Cai [a,*] and Ben Young [b]

[a] Department of Civil Engineering, The University of Hong Kong, Pokfulam Road, Hong Kong

[b] Department of Civil and Environmental Engineering, The Hong Kong Polytechnic University, Hong Kong

(Formerly, Department of Civil Engineering, The University of Hong Kong, Pokfulam Road, Hong Kong)

Abstract

There is presently very limited research work on the mechanical properties of thin sheet steel (TSS) after exposure to high temperatures (at post-fire condition). In this study, 35 coupon specimens were tested after being exposed to high temperatures. The coupon specimens were extracted from three different grades of TSS, namely, grades of G450, G500 and G550, with nominal 0.2% proof stresses (yield strengths) of 450, 500 and 550 in MPa, respectively. The TSS grades G450, G500 and G550 had nominal thicknesses of 1.90, 1.20 and 0.42 mm, respectively. The liquefied petroleum gas (LPG) furnace and the electronic furnace were used to heat the coupon specimens to four different nominal peak temperatures up to 900 °C, where the ISO-834 standard fire curve was followed by the LPG furnace. The specimens were generally soaked before being cooled to ambient temperature conditions inside the furnaces. Tensile coupon tests were conducted on the TSS, where the mechanical properties associated with the stress-strain curves were investigated, including Young's modulus, 0.2% proof stress, ultimate strength, ultimate strain and fracture strain. The residual mechanical properties at post-fire conditions were compared in terms of steel grades, the two different heating methods and the peak temperatures the specimens exposed. Furthermore, the retention factors were compared with those predicted by proposed equations in the literature. New predictive curves are proposed for the determination of the residual mechanical properties of TSS after they were exposed to elevated temperatures. It was demonstrated that the proposed predictive curves are suitable for TSS with nominal 0.2% proof stress ranged from 450 to 550 MPa, and nominal thickness up to 1.90 mm.

Keywords: Coupon tests; high temperatures; residual mechanical properties; retention factor; thin sheet steel.

* Corresponding author. Tel.: +852-2859-2665

E-mail address: yccai@hku.hk (Y. Cai)

1. Introduction

Cold-formed steel has advantages that include a high strength-to-weight ratio, flexibility in fabricating different cross-section shapes, ease in construction [1]. The behavior of cold-formed steel structures under fire conditions has been an issue of particular concern, due to the deterioration of steel mechanical properties at high temperatures. The deterioration of mechanical properties of cold-formed steel at elevated temperatures have been investigated, for example, by Chen and Young [2]. The full process of fire development can be assumed to go through four stages: incipient, growth, burning after flashover, and decay [3]. Structural members will cool down along with the decreasing atmosphere temperature in the last stage. At this stage, the concern is with safety of the structure after exposure to high temperatures (at post-fire conditions), and there is a need to investigate the structural behavior.

In the last few years, significant progress has been made regarding the mechanical properties of carbon steels and stainless steels after exposure to elevated temperatures. For carbon steels, investigations have focused mainly on high strength materials with nominal yield strengths of 460 MPa [4], 690 MPa [4-6], 960 MPa [7], and 700 MPa and 900 MPa [8]. The investigations of post-fire mechanical properties covered different types of stainless steel, including austenitic stainless steel [9-11], ferritic stainless steel [11-12] and duplex stainless steel [11, 13]. The post-fire mechanical properties of thin sheet steel (TSS) grade S355GD+Z with nominal thickness of 2.0 mm was investigated by Outinen [14]. Gunalan and Mahendran [15] recently investigated the post-fire mechanical properties of TSS of G300, G500 and G550, where the nominal thicknesses were 1.00 mm, 1.15 mm and 0.95 mm, respectively. The specimens were cut longitudinally to the rolling direction of steel sheets [14-15]. Predictive curves were proposed for the residual mechanical properties of the steels after exposure to high temperatures up to 800 °C [15].

It should be noted that other factors of mechanical properties, such as the creep effect, would affect the behavior of steel at elevated temperatures [16-17] and also at cooling down stage after exposure to high temperatures. Creep crack initiation and growth at high temperatures limit the life time of steel structures [18]. Creep strains could be basically divided into three stages. In the first stage, the rates of creep decrease with time because of the material strain hardening until a minimum creep rate is achieved [19-20]. Following the secondary stage, there is a balance between strain hardening and thermal softening [21-22], and the rate of

creep was approximately maintained. In the last stage, the rates of creep increase because of thermal softening, damage accumulation, and/or associated net section reduction, until rupture occurs [23]. It is noteworthy that the relatively small differences in chemical composition of material could evidently affect these three stages as discussed by Holdsworth [24]. At high temperatures, in particular, when the temperatures above approximately 400 °C, creep strains become increasingly influential, generally resulting in lower reduction factors being obtained from transient state tests than steady state tests [25]. Tan et al. [26] developed a finite element formulation for the analysis of two-dimensional steel frames either at ambient or elevated temperatures, where the effects of creep were incorporated. The findings indicated that creep generally starts to be dominant on the buckling of heated steel columns when temperatures beyond 400°C. It should be noted that the rate of temperature increases is also an important factor for the effect of creep at high temperatures, with the considerably higher rate of temperature development leads to less significant of creep influent in transient state tests [25]. The creep effects were not considered and investigated in the post-fire mechanical properties of carbon steels and stainless steels after exposure to elevated temperatures [4-15], which could be due to the fact that the coupon specimens were not being loaded during heating and cooling stages. In this study, the creep of the TSS during heating and cooling stages was also not investigated.

Previous research on the mechanical properties of coupon specimens were basically heated with a constant heating rate (e.g., 10 °C/min [8] and 20 °C/min [11]) up to the predetermined peak temperature. It should be noted that the temperature increment of a structure in real fire conditions does not occur at a constant rate. In fact, it could be varied heating rates during the temperature increment process, e.g., the commonly used ISO-834 part 1 standard fire curve for structures in fire [27]. Note that the ISO-834 curve [27] is not the reputed temperature-time relationship for structures under natural fire conditions. However, it should be noted that the ISO-834 curve [27] has not been adopted in the previous investigations [4-15] for the post-fire mechanical properties of steel. In addition, investigations of the residual mechanical properties of TSS after exposure to high temperatures have been relatively limited to date.

In this study, 35 coupon specimens were tested to investigate the mechanical properties that associated with the stress-strain curves of TSS after exposure to elevated temperatures. The coupon specimens were extracted from three different grades of TSS, namely G450, G500

and G550. The three TSS grades had nominal thicknesses of 1.90, 1.20 and 0.42 mm, respectively. The liquefied petroleum gas (LPG) furnace and the electronic furnace were used to heat the coupon specimens to four different nominal peak temperatures up to 900 °C, where the ISO-834 standard fire curve [27] was followed by the LPG furnace. The specimens were generally soaked before cooling down to ambient temperature conditions inside the furnaces. After that, tensile tests were conducted to obtain the stress-strain curves and mechanical properties of the TSS. The residual mechanical properties at post-fire conditions were compared in terms of steel grades, the two different heating methods as well as the peak temperatures to which the specimens were exposed. Furthermore, the retention factors were compared with those predicted by the equations proposed in the literature. New predictive curves for the determination of the residual mechanical properties of TSS, after exposure to elevated temperatures, are proposed.

2. Experimental investigation

2.1. Test specimens

Tensile coupon tests were conducted to investigate the mechanical properties of TSS (G450, G500 and G550) after exposure to high temperatures. The coupon specimens were extracted in the direction parallel to the rolling direction of the steel sheets, namely, in the length direction. The dimensions of the coupon specimen having 25 mm gauge length with 6 mm width [28] were designed in accordance with the AS 2291 [29]. The dimensions of the TSS coupon specimen are illustrated in Figure 1.

2.2. Specimen labelling

The test specimen was labelled such that the nominal sheet thickness (t) and nominal 0.2% proof stress ($f_{0.2}$) could be identified, as shown in Tables 1-3. For example, the label of 042-G550 defines the following test specimen. The first segment indicates the t the coupon specimens, where 042 means t = 0.42 mm. The following segment means the steel grade with the nominal $f_{0.2}$ of the specimens, where G550 had the $f_{0.2}$ = 550 MPa.

2.3. Nominal peak exposed temperatures

The TSS coupon specimens were heated from ambient temperature (20 °C) to a

pre-determined peak temperature and then cooled down to the ambient temperature condition. Four different target peak temperatures were selected for the three different grades of TSS coupon specimens in this study. The selected target peak temperatures were 300 °C, 550 °C, 750 °C and 900 °C. These nominal peak temperatures were selected based on the post-fire mechanical properties of cold-formed high strength steel conducted by Li and Young [8] and those of cold-formed steel conducted by Gunalan and Mahendran [15]. In addition, it should be noted that the coupon specimens without heating and cooling processes were prepared and tested as a direct comparison.

2.4. Heating and cooling methods

2.4.1 General

In this study, two different furnaces were used to heat the TSS coupon specimens. One was the LPG furnace that could heat up to 1200 °C by following various international fire standard curves, e.g., ISO-834 Part-1 standard fire curve [27], and the other was the MTS electric furnace which could provide up to 1400 °C by heating elements with the maximum heating rate of 100 °C/min. Note that the LPG furnace could provide a higher heating rate than the maximum of 100 °C/min produced by the electric furnace.

It should be noted that the research conducted by Li and Young [8] showed that the difference of heating rates between 10 °C/min and 100 °C/min had negligible effects on the mechanical properties of cold-formed high strength steel after being exposed to elevated temperatures. The test results reported by Huang and Young [12] showed that the extent of soaking time had minimum effect on the stress-strain curves of ferritic stainless steel material. In this study, the heating rate of the LPG furnace was set such that the temperature inside followed the temperature-time of the ISO-834 Part 1 standard fire curve [27], while the heating rate of 40-60 °C/min was used in the electric furnace. The coupon specimens were generally soaked for around 15 minutes at the target peak temperature before cooling down to the ambient temperature condition inside the furnaces.

2.4.2. Using liquefied petroleum gas furnace

An LPG furnace with dimensions of 3.0×1.1 m in floor area and 3.0 m in height was used to

simulate the fire conditions in this study. Due to the large spacing of the LPG furnace, the TSS coupon specimens were heated together with other high strength steel tubular members and joints inside the furnace for the same nominal target peak temperatures. The investigation of the high strength steel joints under post-fire condition was reported by Padney and Young [30].

There were nine plate type thermometers installed at various heights to measure the furnace temperature. Eight gas burner openings were installed inside the furnace with four openings on each parallel side, distributed along the furnace height. The gas burner openings could be adjusted independently for uniform heat generation monitored by the nine thermometers. In addition, the furnace heating and pressure could be controlled by using two exhaust openings located near the bottom of the furnace height. The inside furnace was covered by thick thermal ceramic fibre rock wool material for insulation purposes. After closing the furnace door, any marginal openings surrounding it were covered with thick fire-resistant cottons. Details of the LPG furnace were described by Padney and Young [30].

The LPG furnace was then activated by following the ISO-834 standard fire curve [27]. The burning was paused once the average furnace temperature reached the predetermined nominal peak temperature and remained in the paused mode until the temperatures of all the specimens also approached the targeted peak temperature [30]. After around 15 mins of soaking time, the specimens were cooled naturally inside the furnace with very marginal exposure to ambient air from the furnace door until their temperature dropped to around 100 °C. The specimen temperatures measured by K-type nickel-chromium thermocouple for high strength steel tubular joints adjacent to the TSS coupon specimens were reported by Padney and Young [30]. Figure 2 (left) shows the TSS coupon specimens positioned inside the LPG furnace. Figure 3 illustrates the measured temperature-time curves for the four different nominal peak exposed temperatures. The vertical axis plots the furnace temperatures measured by the average readings of thermocouple plates.

2.4.3. Using electrical furnace

An MTS model 653.04 high temperature electric furnace was employed to heat up the TSS coupon specimens to the four different nominal peak temperatures. There were three independent heating chambers located along the height of the furnace at each side. In each

chamber, there was a heating element associated with a thermocouple. Each pair of heating elements could be controlled by the temperature controller. In this study, two additional thermocouples were mounted on the surface of the coupon specimen in order to measure the real-time temperature of the specimen.

Fire-resistant cottons were used to fill any gaps after the closure of the electric furnace. The heating program was designed carefully so there was a minimum overshoot when reaching the nominal peak temperature in the furnace. For the sake of this, the primary peak temperature set in the program of the heating step was a little bit lower than the predetermined nominal peak temperature. When the heating step was completed, the temperature inside the furnace was adjusted manually by the temperature controller of each chamber until the readings from the thermocouples reached the nominal target temperature. After around 15 minutes soaking time, the furnace was deactivated and the specimen inside the furnace was cooled down naturally until the measured temperature was less than 50 °C. It should be noted that the electric furnace was not open during the whole process of heating and cooling. The setup of the TSS coupon specimen heated by the electric furnace is illustrated in Figure 2 (right). Figure 4 illustrates the measured temperature-time curves of the TSS coupon specimens.

2.5. Testing specimens

The coupon specimens were then taken out carefully from the furnaces. The 1:1 hydrochloric acid was used to remove the galvanized zinc coating of the specimens such that the base metal thickness of the specimens was obtained. The base metal thickness and width at the gauge length of the specimens were measured by calibrated micrometer and vernier calliper, respectively. Figure 5 illustrates the gauge length part with coating removed for the two specimens of 120-G500.

An MTS material testing machine was employed to conduct the tensile coupon tests. All the post-fire tensile coupon tests were conducted at ambient temperature conditions. Two strain gauges were attached in the middle of the gauge length at each side, where the measured average values were used to determine the Young's modulus of the specimen. In addition, a calibrated MTS extensometer with a limitation of ± 12.5 mm movement was used to measure the longitudinal strains of the coupon specimens, where the measurements were used to

determine the mechanical properties of the specimen, except for the Young's modulus. The tests were conducted by displacement control with a constant loading rate of 0.2 mm/min until the specimens fractured. A data acquisition system was used to record the loads as well as the readings of the strain gauges and extensometer at regular intervals. Figure 6 illustrates the test setup of the TSS coupon Specimen 120-G500.

3. Stress-strain curves from tests

The stress-strain curves of the TSS coupon specimens after exposure to high temperatures by using the LPG furnace are shown in Figures 7-9, for Series 042-G550, Series 120-G500 and Series 190-G450, respectively. Similarly, those specimen series that using electric furnace are shown in Figures 10-12. In each stress-strain curve, the initial elastic part was plotted by the average readings from the two strain gauges, and the rest was plotted by the measurements from the extensometer. Due to the much larger fracture strains of the specimens after exposure to higher peak temperatures, e.g., 900 °C, the whole stress-strain curves of these specimens without exposure to any high temperature or to lower peak temperatures are not shown in a clear scale in the figures. Therefore, for each series of stress-strain curves, the initial parts were plotted by following the whole stress-strain curves in a separate figure, as shown in Figures 7(b), 8(b), 9(b), 10(b), 11(b) and 12(b).

The mechanical properties that associated with the stress-strain curves of TSS, including the Young's modulus (E), 0.2% proof stress ($f_{0.2}$), 0.5% proof stress ($f_{0.5}$), 1.0% proof stress ($f_{1.0}$), 1.5% proof stress ($f_{1.5}$), 2.0% proof stress ($f_{2.0}$), ultimate strength (f_u), ultimate strain (ε_u) and fracture strain (ε_f), obtained from the tensile coupon tests without exposure to high temperature, are summarized in Table 1. Correspondingly, the mechanical properties of these specimen series after exposure to high temperatures are presented in Tables 2 and 3, including the E_P, $f_{0.2,P}$, $f_{0.5,P}$, $f_{1.0,P}$, $f_{1.5,P}$, $f_{2.0,P}$, $f_{u,P}$, $\varepsilon_{u,P}$ and $\varepsilon_{f,P}$. The nominal peak temperature (T) levels and the measured temperature ranges (T_m) during soaking time to which the specimens exposed are also presented. The definition of the symbols for the mechanical properties shown in Tables 2-3 is illustrated in a stress-strain curve in Figures 13, by Specimen 190-G450 after exposure to 500 °C in the LPG furnace. Figure 14 shows the failure mode of the coupon specimens for the Series of 042-G550, 120-G500 and 190-G450 after the tensile tests.

Generally, there was a sudden load drop at the initial part (corresponding to strain less than 0.5%) of the stress-strain curves for some of the specimens. These sudden drops associated with the peaks are shown in the initial parts of the stress-strain curves in Figures 7-12. The values of the stress at these peaks with the corresponding strains are shown in Tables 2-3; they were close or higher compared to the ultimate strength (f_u and $f_{u,P}$) but occurred at the strain smaller than 0.005 in the stress-strain curves. It should be noted that these stress values were not taken as the ultimate strengths (f_u and $f_{u,P}$) of the test results. These sudden drops could also be found in the stress-strain curves of steel grades of G300, G500 and G550 in Gunalan and Mahendran [15]. Generally, the ductility of the TSS materials was enhanced after exposure to high temperatures. The significant enhancement was found after exposure to temperatures above 750 °C. These will be discussed further in the latter section of this paper.

4. Mechanical properties from test results

4.1. General

The effects of furnaces (different heating and cooling processes) and temperature on the mechanical properties of TSS are discussed in this section. It should be noted that the mechanical properties were obtained based on the stress-strain curves of the TSS. The retention factors of the mechanical properties after exposure to high temperatures were determined from the ratio of the residual mechanical properties (shown in Tables 2-3) over the corresponding mechanical properties (shown in Table 1) without exposure to high temperatures, namely, the retention factors of E_P/E, $f_{0.2,P}/f_{0.2}$, $f_{u,P}/f_u$, $\varepsilon_{u,P}/\varepsilon_u$ and $\varepsilon_{f,P}/\varepsilon_f$. The values of retention factors were plotted and compared with the predictive equations proposed by Gunalan and Mahendran [15] for cold-formed steel, and Li and Young [8] for cold-formed high strength steel, after exposure to elevated temperatures, as shown in Figures 15-19. In the figures, the specimens heated and cooled in the LPG furnace and electric furnace are indicated by "(g)" and "e", respectively. It should be noted that the G300 was defined as low grade steel, while G500 and G550 were defined as high grade steel by Gunalan and Mahendran [15].

4.2. Influence of heating and cooling in furnaces

Generally, the retention factors resulting from the specimens for the two furnaces showed a similar trend after exposure to high temperatures. The differences between the retention factors obtained by the specimens in the LPG furnace and electric furnace under the same

post-fire temperature were generally small. However, the retention factors for the specimens exposed to nominal peak temperature of 550 °C were relatively scattered, for example the retention factors of $f_{0.2,P}/f_{0.2}$ and $f_{u,P}/f_u$ for both specimen series of 042-550 and 120-500, and the retention factor of $\varepsilon_{u,P}/\varepsilon_u$ and $\varepsilon_{f,P}/\varepsilon_f$ for specimen Series 042-550. This may have been due to the mechanical properties of the TSS grades of G500 and G550 being relatively more sensitive after exposure to peak temperatures around 550 °C. Similar scattered results around 550 °C were shown by Gunalan and Mahendran [15] for specimen series 095-G550 and 110-G500, as plotted in Figures 20-22. Furthermore, the actual peak temperatures at the gauge length for specimens in the LPG furnace may be slightly different from the nominal peak temperatures, due to the relatively larger space of the LPG furnace.

4.3. Young's modulus

Generally, as shown in Figure 15, the retention factors of E_P/E for the TSS grade G450 were higher than those of grades G500 and G550 after exposure to high temperatures, in particular when the specimens were exposed to peak temperatures exceeding 550 °C. The retention factors of TSS grade G500 were generally higher than those of the G550 after exposure to elevated temperatures. The three different grades of TSS regained more than 0.95 and 0.92 of the E after exposure to temperatures up to 300 °C and 550 °C, respectively. Generally, the TSS grades of G450, G500 and G550 could regain over 0.93, 0.87 and 0.80 of the E after exposure to temperatures up to 900 °C, respectively.

The predictive curve proposed by Gunalan and Mahendran [15] for low grade steel was found to be unconservative for the retention factors of the three different grades of TSS, while the predictive curve for high grade steel [15] was either conservative for the retention factors of series 120-G450 and 190-G450 or unconservative for those of Series 042-G550 in this study. Furthermore, it should be noted that these predictive curves were applicable for post-fire temperatures up to 800 °C only. It was also found that the predictive curve by Li and Young [8] was generally too conservative for post-fire temperatures above 750 °C for the three different grades of TSS in this study.

4.4. 0.2% proof stress

Generally, as shown in Figure 16, the retention factors of $f_{0.2,P}/f_{0.2}$ for the three different grades

of TSS dropped steadily for the post-fire temperatures up to 550 °C. There was a rapid deterioration for the post-fire temperature ranging from 550 °C to 750 °C. For example, the retention factor for the TSS series 042-550, 120-500 and 190-450 had a maximum drop from 0.80 to 0.30, from 0.95 to 0.41 and from 0.91 to 0.38, respectively. It can also be seen that the retention factors were more scattered at the post-fire temperature of 550 °C than those under other post-fire temperatures, for the TSS series 042-550 and 120-500. Generally, the retention factors of TSS series 120-500 and 190-450 were larger than those of the specimen series 042-550, which means that the 120-500 and 190-450 regained higher percentages of $f_{0.2}$ than those of specimen Series 042-550 under different post-fire temperatures. Overall, the TSS grades of G450, G500 and G550 could regain at least 0.37, 0.32 and 0.30 of the $f_{0.2}$ after exposure to temperatures up to 900 °C in this study.

The predictive curve by Gunalan and Mahendran [15] for low grade steel was generally found to be unconservative for the retention factors of the three different grades of TSS when the post-fire temperatures exceeded 550 °C, while the predictive curve for the high grade steel [15] could generally predict the trends of retention factors for the three different grades of TSS, but up to 800 °C only. It was also found that the predictive curve developed by Li and Young [8] was generally unconservative for post-fire temperatures ranging from 300 to 750 °C for the three different grades of TSS in this study.

4.5. Ultimate strength

Similar to the retention factors of $f_{0.2,P}/f_{0.2}$, the factors of $f_{u,P}/f_u$ dropped steadily for the post-fire temperatures up to 550 °C, followed by a rapid deterioration in the temperatures ranging from 550 to 750 °C, as shown in Figure 17. The retention factor for the TSS series 042-550, 120-500 and 190-450 had a maximum drop from 0.78 to 0.38, from 0.96 to 0.50 and from 0.93 to 0.57, respectively. In addition, the retention factors for the TSS series 042-550 and 120-500 were more scattered at the post-fire temperature of 550 °C than those under other post-fire temperatures. Generally, the retention factors of TSS series 120-500 and 190-450 were larger than those of specimen Series 042-550, which means that specimen series 120-500 and 190-450 regained higher percentages of f_u than those of specimen Series 042-550 under different post-fire temperatures. Overall, the TSS grades of G450, G500 and G550 could generally regain at least 0.53, 0.45 and 0.38 of the f_u after exposure to temperatures up to 900 °C.

The predictive curve for the retention factors of $f_{u,P}/f_u$ developed by Gunalan and Mahendran [15] for low grade steel, was generally unconservative for the retention factors of TSS under the different post-fire temperatures, while the predictive curve for high grade steel could generally predict the trends of retention factors for the three different grades of TSS, but was unconservative for the post-fire temperature of 300 °C, and the curve was applicable up to 800 °C only. Generally, the predictive curve proposed by Li and Young [8] could predict the trend of retention factors, but the predictions are unconservative for specimen series 042-550 and 120-500 at different post-fire temperatures.

4.6. Ultimate strain and fracture strain

On the contrary to those of the $f_{0.2,P}/f_{0.2}$ and $f_{u,P}/f_u$, it can be observed that the values of the $\varepsilon_{u,P}/\varepsilon_u$ and $\varepsilon_{f,P}/\varepsilon_f$ generally increase as the exposed temperatures increased, with a more significant increment when the exposed temperatures exceeded 550 °C, for the three different grades of TSS materials, as shown in Figures 18-19. There a drastic increment in the values of both $\varepsilon_{u,P}/\varepsilon_u$ and $\varepsilon_{f,P}/\varepsilon_f$ for specimen Series 042-550 when the temperatures were over 550 °C. The values of both $\varepsilon_{u,P}/\varepsilon_u$ and $\varepsilon_{f,P}/\varepsilon_f$ for specimen Series 042-550 were higher than those of the specimen series 120-500 and 190-450 at different post-fire temperatures. This may be due to the values of both ε_u and ε_f being relatively much smaller for Specimen 042-550 without exposure to high temperatures. The values of both $\varepsilon_{u,P}/\varepsilon_u$ and $\varepsilon_{f,P}/\varepsilon_f$ for specimen Series 120-500 were generally higher than those of specimen Series 190-450 at the same post-fire temperatures. The values of the fracture strain (ε_f and $\varepsilon_{f,P}$) can reflect the ductility of the TSS materials, with the higher value indicating the better ductility. Therefore, the increment of $\varepsilon_{f,P}/\varepsilon_f$ corresponding to the increment of post-fire temperature indicates that the ductility of the three different grades of TSS material was generally increased after exposure to elevated temperatures, with a significant increment above the post-fire temperature of 750 °C.

The factors of ultimate strain ($\varepsilon_{u,P}/\varepsilon_u$) and fracture strain ($\varepsilon_{f,P}/\varepsilon_f$) were not reported and there is no proposed predictive curve shown by Gunalan and Mahendran [15], therefore, only the predictive curves proposed by Li and Young [8] were compared, as shown in Figures 18-19. Note that the proposed equations for the factors of $\varepsilon_{u,P}/\varepsilon_u$ in Li and Young [8] were based on the investigations of cold-formed high strength steel grades S700 and S900, while the proposed equations for the factors of $\varepsilon_{f,P}/\varepsilon_f$ in Li and Young [8] were based on not only the

results of the steel grades S700 and S900, but also those of hot-rolled steel grade Q690 [4]. The predictive curves for the factors of $\varepsilon_{u,P}/\varepsilon_u$ and $\varepsilon_{f,P}/\varepsilon_f$ were generally found to be conservative.

5. Predictive curves for residual mechanical properties

5.1. General

As discussed in Section 4 of this paper, the curves proposed by Gunalan and Mahendran [15] and Li and Young [8] generally could not accurately and safely predict the retention factors of the mechanical properties of the three different grades of TSS after exposure to elevated temperatures. The curves proposed by Li and Young [8] generally provided conservative and safe predictions for the factors of $\varepsilon_{u,P}/\varepsilon_u$ and $\varepsilon_{f,P}/\varepsilon_f$ for the three different grades of TSS after exposure to elevated temperatures. Therefore, in this study, new predictive curves to determine the residual mechanical properties (E_P, $f_{0.2,P}$ and $f_{u,P}$) of the TSS after exposure to elevated temperatures are proposed, as shown in Figures 20-22. The data for the TSS grades 042-G550, 120-G500 and 190-G450 obtained in this study, and those for the sheet steel grades 095-G550 and 110-G500 reported by Gunalan and Mahendran [15], were employed to propose the retention factors. Therefore, the predictive curves proposed in this study can be applied for TSS with $f_{0.2}$ ranged from 450 to 550 MPa, and thicknesses up to 1.90 mm.

The unified equation, as shown in Equation (1), which was proposed by Chen and Young [2] for residual material properties of stainless steels at elevated temperatures, was employed in this study. The numbers of data employed to derive the proposed retention factors are summarized in Table 4. The coefficients of equations for the retention factors of the Young's modulus, 0.2% proof stress and ultimate strength of TSS after exposure to elevated temperatures are detailed in the following sub-sections.

$$k = a - \frac{(T-b)^n}{c} \tag{1}$$

where k is the retention factor, a, b, c and n are the coefficients related to mechanical properties and temperatures, T is the post-fire peak temperature in degree Celsius (°C).

5.2. Young's modulus

The retention factor ($k_E = E_P/E$) of the Young's modulus for the different grades of TSS have been plotted in Figure 20. It can be seen that the specimen series 095-G550, 115-G500, 120-G500 and 190-G450 regained 98% of the E after exposed to temperature up to 500 °C, beyond which the deterioration of the E_P became relatively more severe, especially for specimen series 095-G550 and 120-G500. For the specimen Series 042-550, the deterioration of the E_P developed relatively steadily up to the post-fire temperature of 550 °C, then followed a significant deterioration for the temperature ranged from 550 to 750 °C. In this study, a curve for the retention factor (k_E) of E/E_P was proposed. Generally, the proposed curve could capture the reduction trend of Young's modulus for the different grades of TSS after exposure to high temperatures. The coefficients for k_E in the unified Equation (1) are presented in Table 5.

5.3. 0.2% proof stress

Figure 21 shows the retention factor ($k_{0.2} = f_{0.2,P}/f_{0.2}$) of the 0.2% proof stress for the different grades of TSS. The specimen series regained 98% of their $f_{0.2}$ after exposure to temperatures up to 300 °C, beyond which there was a drastic deterioration of $f_{0.2,P}$ in the post-fire temperatures ranging from 500 to 600 °C. The deterioration of the $f_{0.2,P}$ became relatively small in the post-fire temperature ranged from 750 to 900 °C while, for the specimen Series 042-550, there was a relatively obvious deterioration of the $f_{0.2,P}$ for the post-fire temperature up to 300 °C. A significant deterioration followed for the temperatures ranging from 300 to 750 °C. The deterioration of the $f_{0.2,P}$ became smaller as those of other TSS in the post-fire temperatures ranging from 750 to 900 °C. Similarly, a curve for the retention factor ($k_{0.2}$) of $f_{0.2,P}/f_{0.2}$ was proposed to capture the reduction trends of the TSS specimens after exposure to high temperatures, as shown in Figure 21. The coefficients for $k_{0.2}$ in the unified Equation (1) are presented in Table 5.

5.4. Ultimate strength

Figure 22 shows the retention factor ($k_u = f_{u,P}/f_u$) of the ultimate strength for the different grades of TSS. Similarly to the $k_{0.2}$, the specimen series regained 97% of their ultimate strength (f_u) after exposure to peak temperatures up to 300 °C, beyond which there was a

drastic deterioration of $f_{u,P}$ in the post-fire temperature ranging from 500 to 600 °C. The deterioration of the $f_{u,P}$ became relatively small in the post-fire temperatures ranging from 600 to 900 °C. In addition, the retention factor of k_u for specimen Series 042-550 showed an obvious deterioration for the post-fire temperature up to 300 °C, followed by a more significant deterioration up to the post-fire temperature of 550 °C. The deterioration of the $f_{u,P}$ became smaller as those of other TSS in the post-fire temperatures ranging from 550 to 900 °C. Similarly, a curve for the retention factor (k_u) of $f_{u,P}/f_u$ was proposed to capture the reduction trends of the TSS specimens after exposure to high temperatures, as shown in Figure 22. The coefficients for k_u in the unified Equation (1) are presented in Table 5.

6. Conclusions

In this study, 35 coupon specimens were tested to investigate the mechanical properties of thin sheet steel (TSS) after exposure to high temperatures. The mechanical properties were obtained from the stress-strain curves of TSS by coupon tests. The coupon specimens were extracted from TSS grades of G450, G500 and G550 with nominal thicknesses of 1.90, 1.20 and 0.42 mm, respectively. The liquefied petroleum gas (LPG) furnace and the electronic furnace were used to heat the coupon specimens to four nominal peak temperatures of 300 °C, 550 °C, 750 °C and 900 °C.

Tensile coupon tests were then conducted to obtain the mechanical properties that associated with the stress-strain curves of the TSS after exposure to elevated temperatures. The residual mechanical properties obtained from the tests were compared. The differences between the retention factors obtained by the specimens in the LPG furnace and electric furnace under the same post-fire temperature were generally minor. The TSS grades of G450, G500 and G550 could regain over 0.93, 0.87 and 0.80 of their Young's modulus after exposed to temperatures up to 900 °C, respectively. There was a rapid deterioration of $f_{0.2}$ and f_u in the temperatures ranging from 550 to 750 °C. After exposure to temperatures up to 900 °C, the TSS grades of G450, G500 and G550 could regain at least 0.37, 0.35 and 0.30 of the $f_{0.2}$, respectively, and regained at least 0.53, 0.45 and 0.38 of the f_u, respectively.

The retention factors were compared with the predictive curves in the literature. Overall, those in the literature were not found to be suitable to predict the residual mechanical properties of TSS after exposure to elevated temperatures in this study. New predictive curves are proposed

for the retention factors of E, $f_{0.2}$ and f_u of the TSS, where the post-fire mechanical properties of sheet steel grades G500 and G550 reported by Gunalan and Mahendran [15] were also used. The new proposed predictive curves are found to be suitable for the residual mechanical properties of TSS after exposure to elevated temperatures, where TSS had the nominal 0.2% proof stress ranging from 450 to 500 MPa, and nominal thicknesses up to 1.90 mm.

Acknowledgments

The authors are grateful to BlueScope Lysaght (Singapore) Pte. Ltd. for supplying the test specimens. The authors are also thankful to Mr. Fan FEI for his assistance in the experimental program as part of his final year undergraduate research project at The University of Hong Kong. The research work described in this paper was supported by a grant from the Research Grants Council of the Hong Kong Special Administrative Region, China (Project No. HKU719711E).

References

[1] L. Wang, B. Young, Design of cold-formed steel channels with stiffened webs subjected to bending, Thin-Walled Structures 2014. 85, 81-92

[2] J. Chen B. Young, Experimental investigation of cold-formed steel material at elevated temperatures. Thin-Walled Structures 2007. 45, 96-110.

[3] A. H. Buchanan, Structural design for fire safety, John Wiley & Sons Ltd., West Sussex, 2001.

[4] X. Qiang, F.S. Bijlaard, H. Kolstein, Post-fire mechanical properties of high strength structural steels S460 and S690, Engineering Structures 2012. 35, 1-10.

[5] G-Q Li, H. Lyu, C. Zhang, Post-fire mechanical properties of high strength Q690 structural steel. Journal of Constructional Steel Research 2017. 132, 108-116.

[6] S.P. Chiew, M.S. Zhao, C.K. Lee, Mechanical properties of heat-treated high strength steel under fire/post-fire conditions, Journal of Constructional Steel Research 2014. 98, 12-19.

[7] X. Qiang, F.S. Bijlaard, H. Kolstein, Post-fire performance of very high strength steel S960, Journal of Constructional Steel Research 2013. 80, 235-242.

[8] H.T. Li, B. Young, Residual mechanical properties of high strength steels after exposure to fire, Journal of Constructional Steel Research 2018. 148, 562-571.

[9] X.Q. Wang, Z. Tao, T.Y. Song, L.H. Han, Stress-strain model of austenitic stainless steel after exposure to elevated temperatures, J. Constr. Steel Res 2014. 99, 129–139.

[10] X. Gao, X. Zhang, H. Liu, Z. Chen, H. Li, Residual mechanical properties of stainless steels S30408 and S31608 after fire exposure, Construction and Building Materials 2018. 165, 82-92.

[11] Z. Tao, X.Q. Wang, M. K. Hassan, T.Y., Song, L. A. Xie, Behaviour of three types of stainless steel after exposure to elevated temperatures. Journal of Construction Steel Research 2019. 152, 296-311.

[12] Y. Huang, B. Young, Post-fire behaviour of ferritic stainless steel material, Construction and Building Materials 2017. 157, 654-667.

[13] Y. Huang, B. Young, Material properties of lean duplex stainless steel at post-fire condition, Thin-Walled Structures 2018. 130, 564-576.

[14] J. Outinen, P. Mäkeläinen, Mechanical properties of structural steel at elevated temperatures and after cooling down, Fire and Materials 2004. 28, 237-251.

[15] S. Gunalan, M. Mahendran, Experimental investigation of post-fire mechanical properties of cold-formed steels, Thin-Walled Structures 2014. 84, 241-254.

[16] S.L. Mannan, M. Valsan. High-temperature low cycle fatigue, creep－fatigue and thermomechanical fatigue of steels and their welds. International Journal of Mechanical Sciences 2006, 48, 160-175.

[17] K. Maciejewski, Y. Sun, O. Gregory, H. Ghonem. Time-Dependent Deformation of Low Carbon Steel at Elevated Temperatures Materials Science and Engineering: A 2012, 534, 147-156.

[18] C. M. Davies. Predicting creep crack initiation in austenitic and ferritic steels using the creep toughness parameter and time-dependent failure assessment diagram. Fatigue Fracture of Engineering Materials and Structures 2009, 32, 820–836.

[19] R.W., Bailey. Note on the softening of strain hardened metals and its relation to creep. Journal of the Institute of Metals 1926, 35, 27-40.

[20] E. Orowan. The creep of metals. Journal of the West if Scotland Iron and Steel Institute 1946, 54, 45-53.

[21] F.H. Norton. Creep of Steel at High Temperatures; McGraw-Hill: New York, NY, USA, 1929.

[22] J. Weertman. Theory of steady-state creep based on dislocation climb. Journal of Applied Physics 1955, 26, 1213-1217.

[23] H. Riedel. Fracture at High Temperatures; Springer: Berlin/Heidelberg, Germany, 1987.

[24] S. Holdsworth. Creep-Ductility of High Temperature Steels: A Review. Metals, 2019, 9(3), 342.

[25] L. Gardner, A. Insausti, K.T. Ng, M. Ashraf. Elevated temperature material properties of stainless steel alloys. Journal of Constructional Steel Research 2010, 66, 634-647

[26] K. H. Tan, S. K. Ting and Z. F. Huang. Visco-Elasto-Plastic Analysis of Steel Frames in Fire. Journal of Structural Engineering 2002, 128(1): 105-114.

[27] Fire-resistance tests - Elements of Building Construction - Part 1 - General requirements. ISO 834-1, International Organization of Standards, 1999.

[28] Y. Cai, B. Young, Behavior of cold-formed stainless steel single shear bolted connections at elevated temperatures, Thin-Walled Structures 2014. 75, 63-75.

[29] AS 2291. Methods for the Tensile Testing of Metals at Elevated Temperatures, Standards Australia, Sydney, Australia, 1979.

[30] M. Pandey, B. Young, Post-fire behaviour of cold-formed high strength steel tubular X-joints subjected to ISO-834 standard fire, Proceedings of International Conference on Engineering Research and Practice for Steel Construction 2018 (ICSC2018), Paper No. 197, Hong Kong, China.

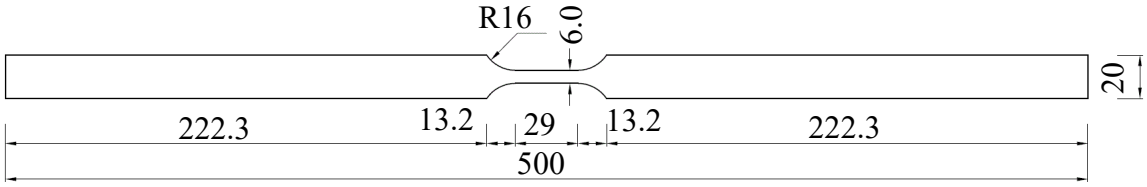

Figure 1: Dimensions (in mm) of TSS coupon specimen

Figure 2: Coupon specimens heated in LPG furnace (left) and in electric furnace (right)

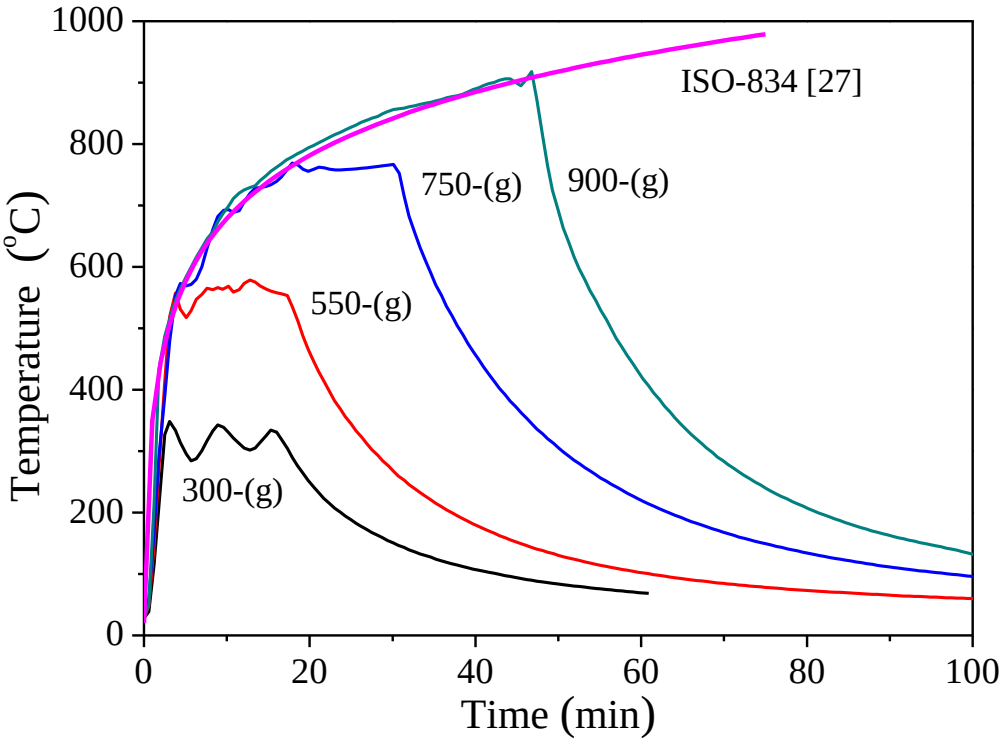

Figure 3: Measured temperature-time curves for TSS specimens in LPG furnace

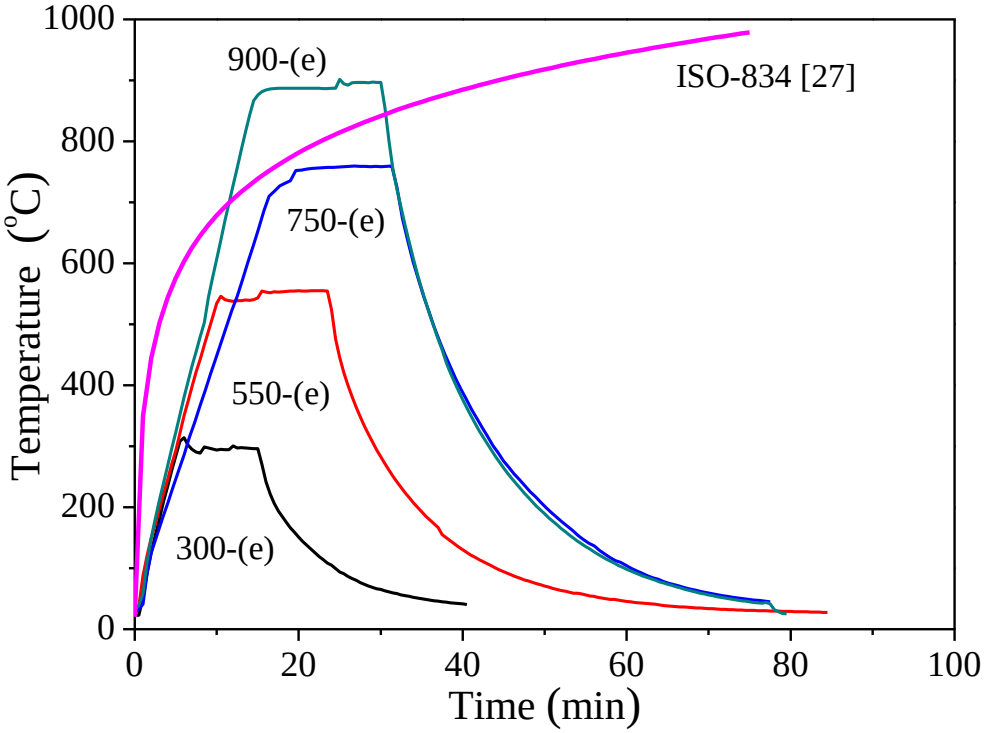

Figure 4: Measured temperature-time curves of TSS specimens in electrical furnace

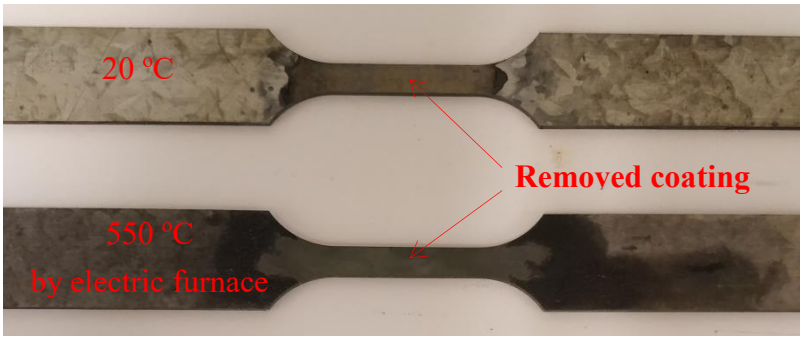

Figure 5: Coupon specimens of Series 120-G500 after coating removed at gauge length part

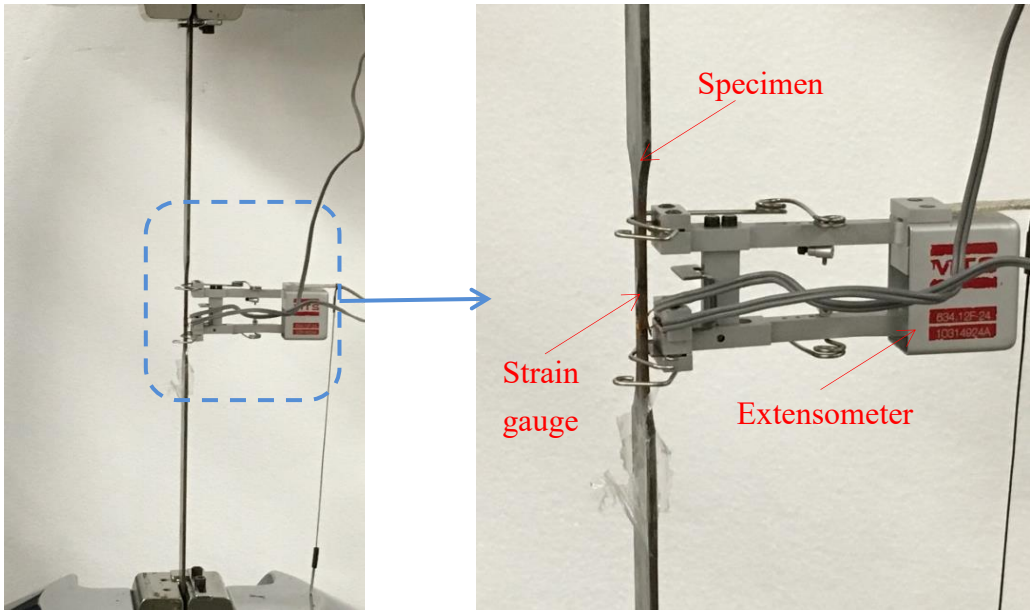

Figure 6: Test setup of TSS coupon Specimen 120-G500

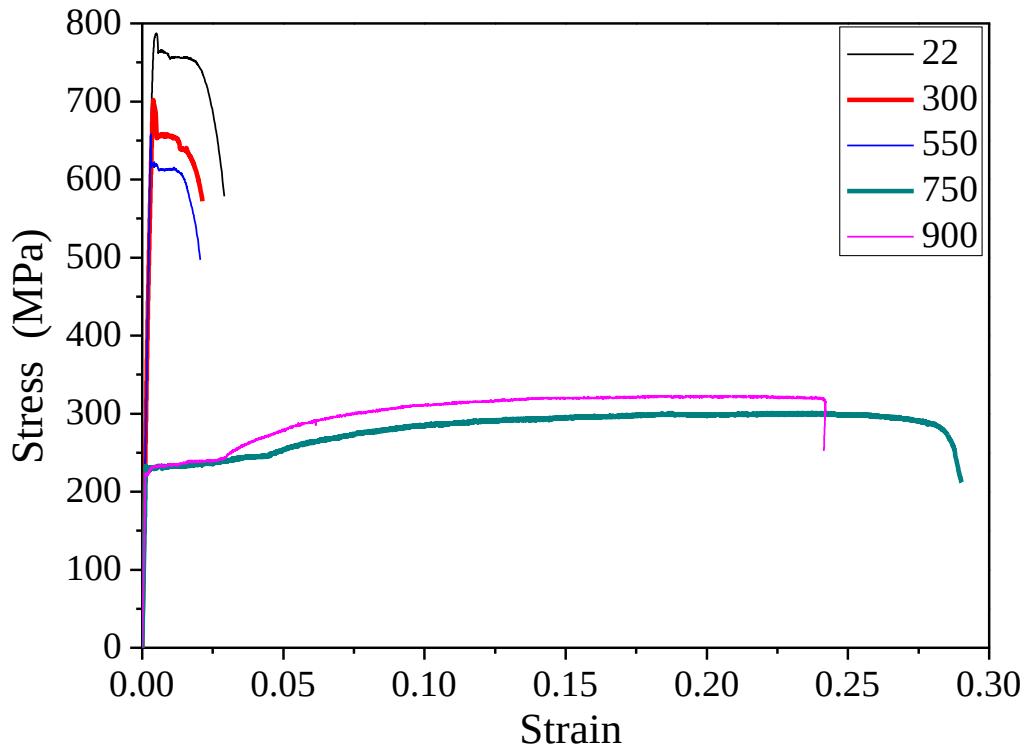

a) Complete curves

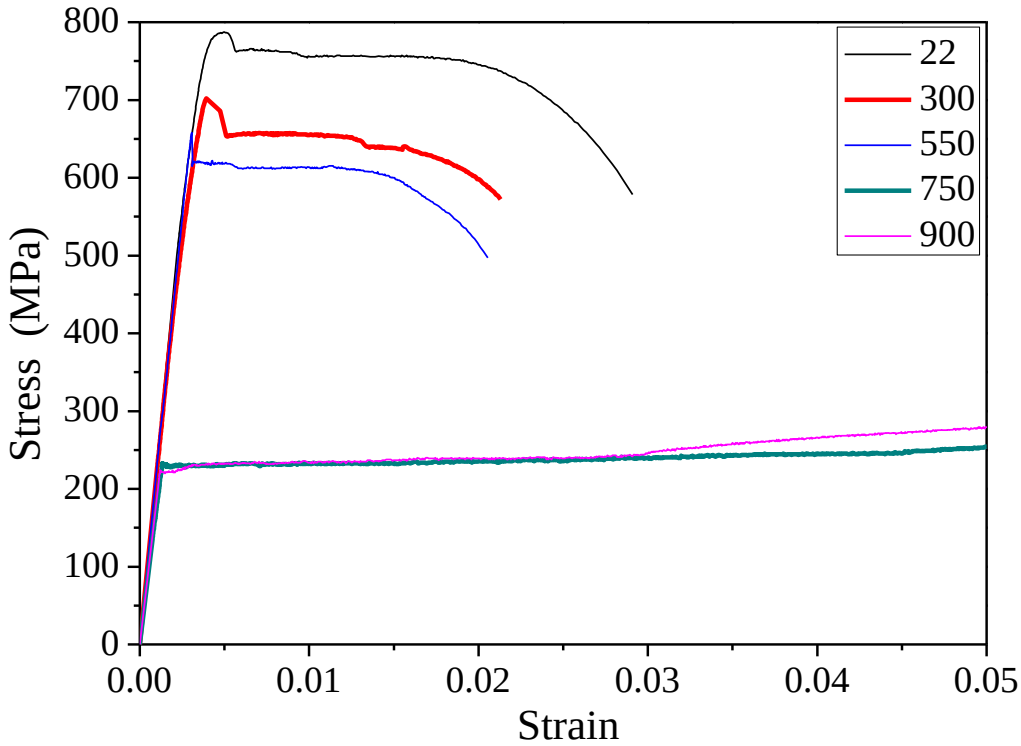

b) Initial parts of complete curves

Figure 7: Stress-stain curves of Series 042-G450 by LPG furnace

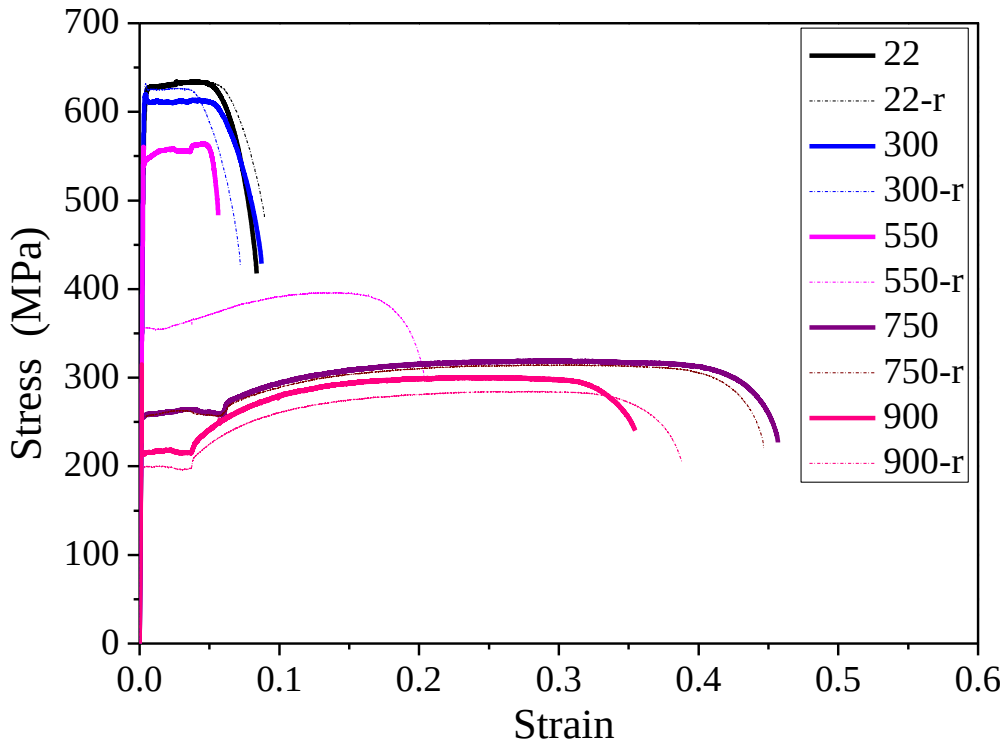

a) Complete curves

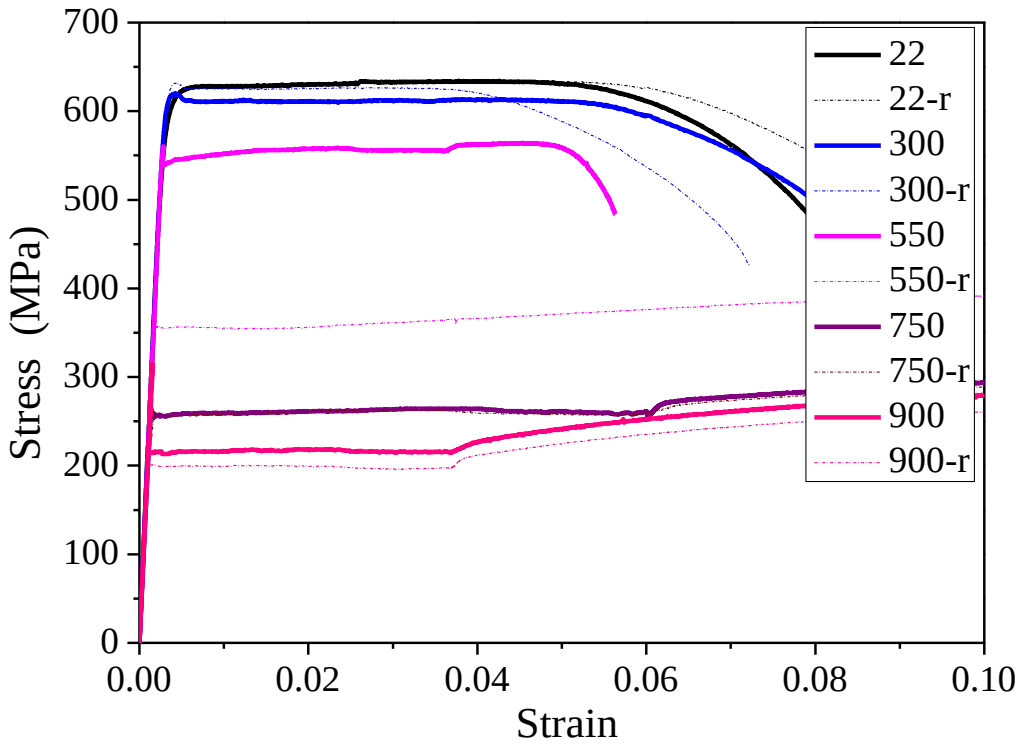

b) Initial parts of complete curves

Figure 8: Stress-stain curves of Series 120-G500 by LPG furnace

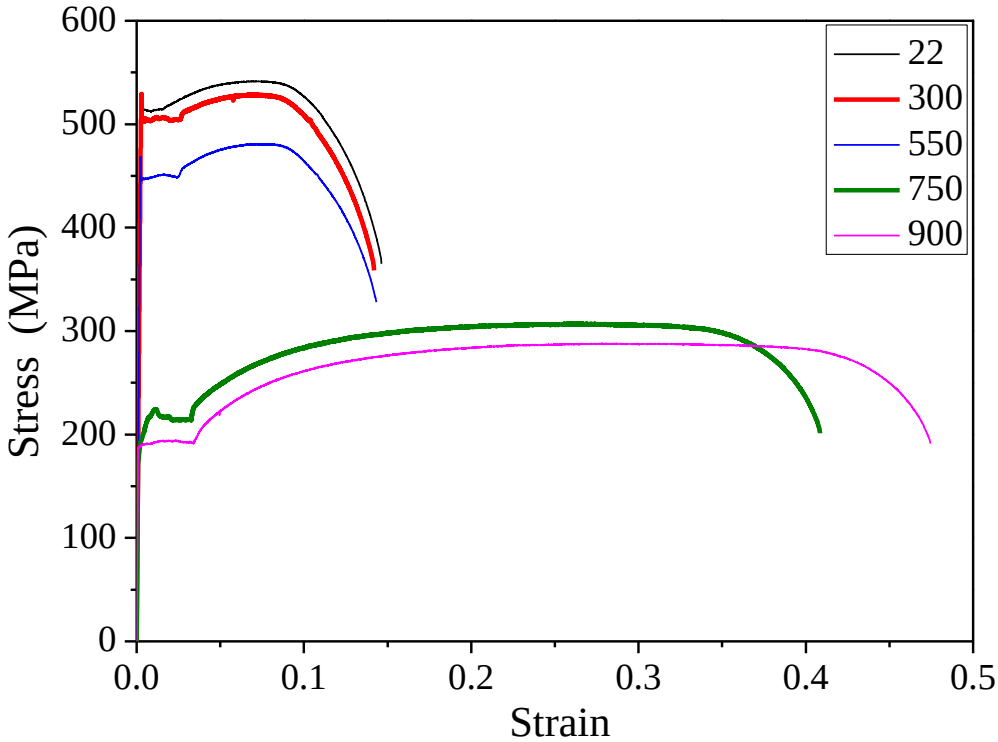

a) Complete curves

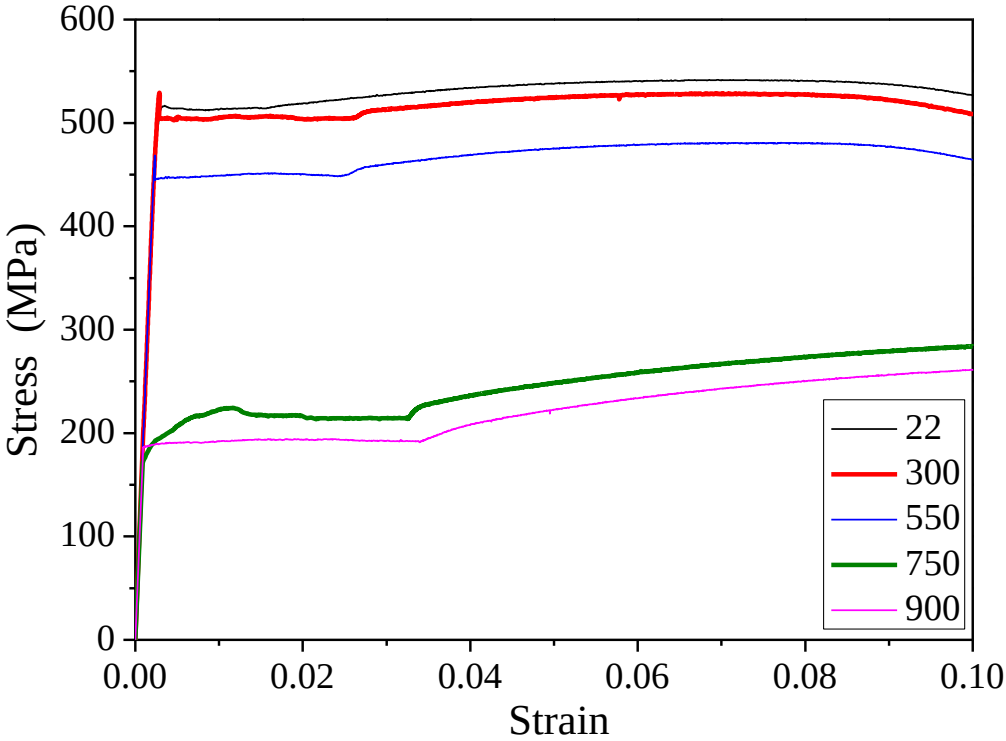

b) Initial parts of complete curves

Figure 9: Stress-stain curves of Series 190-G450 by LPG furnace

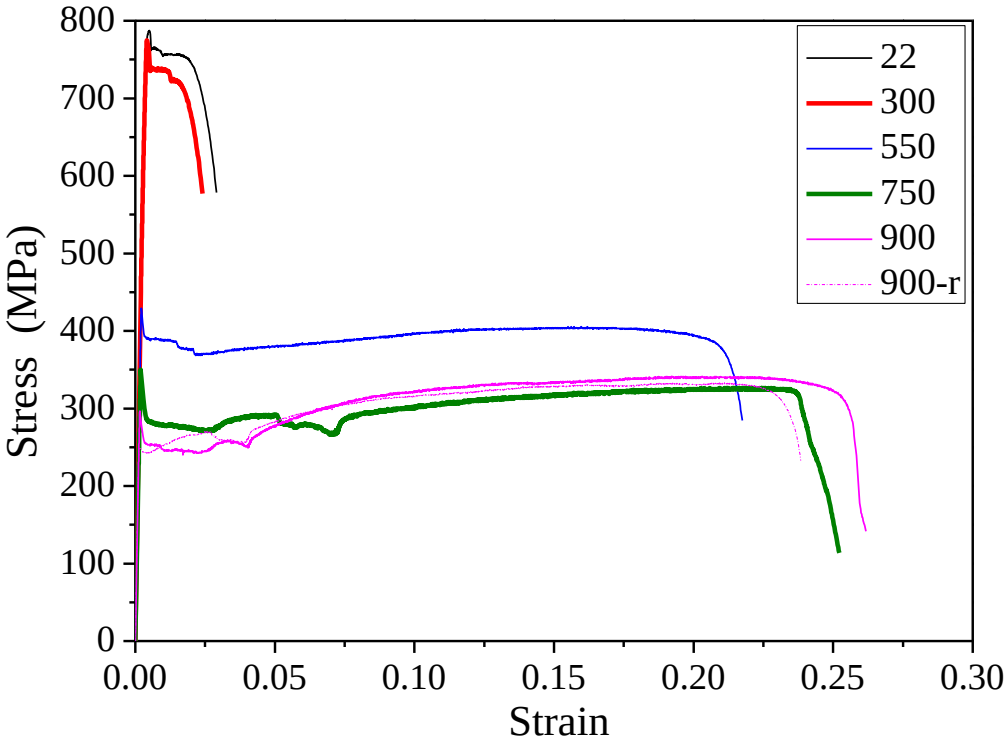

a) Complete Curves

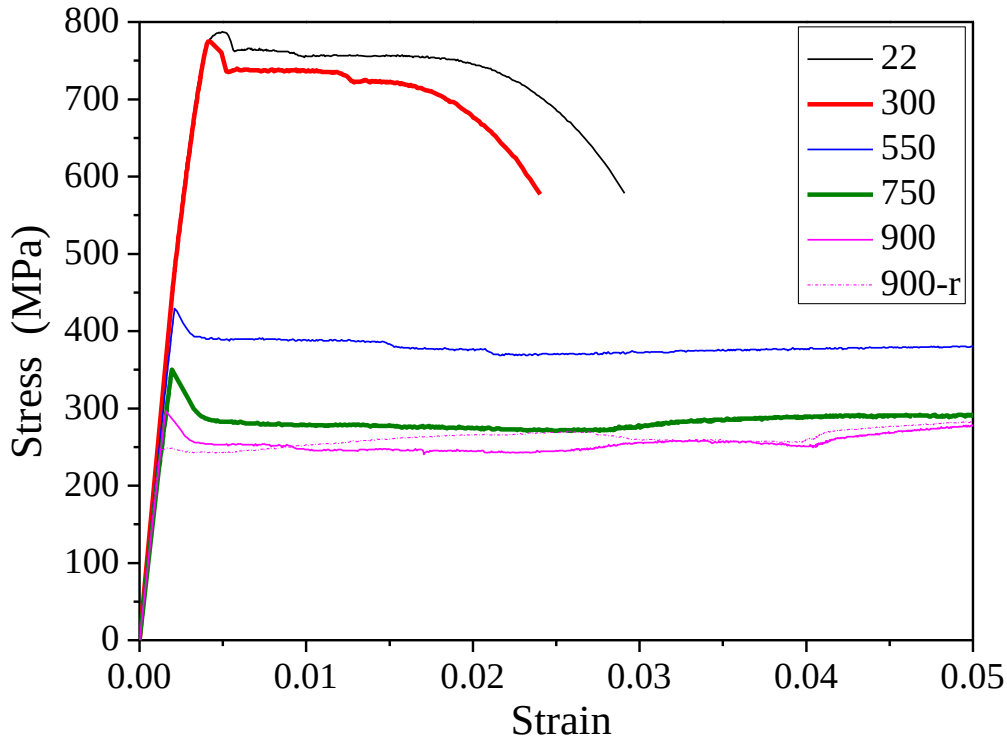

b) Initial parts of complete curves

Figure 10: Stress-stain curves of Series 042-G550 by electric furnace

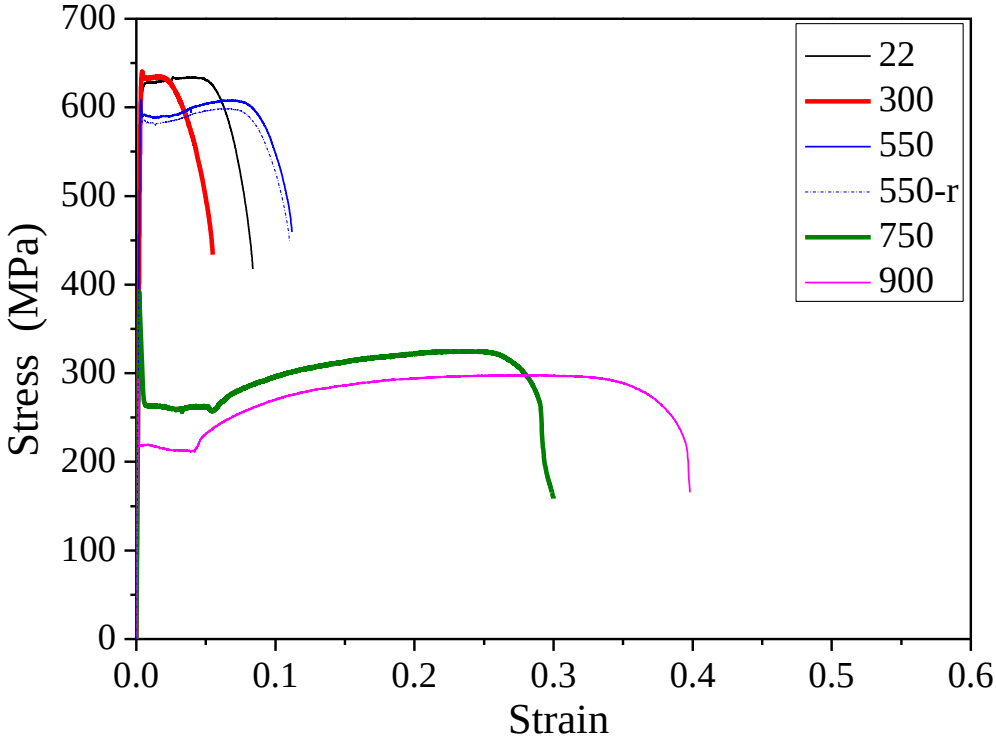

a) Complete curves

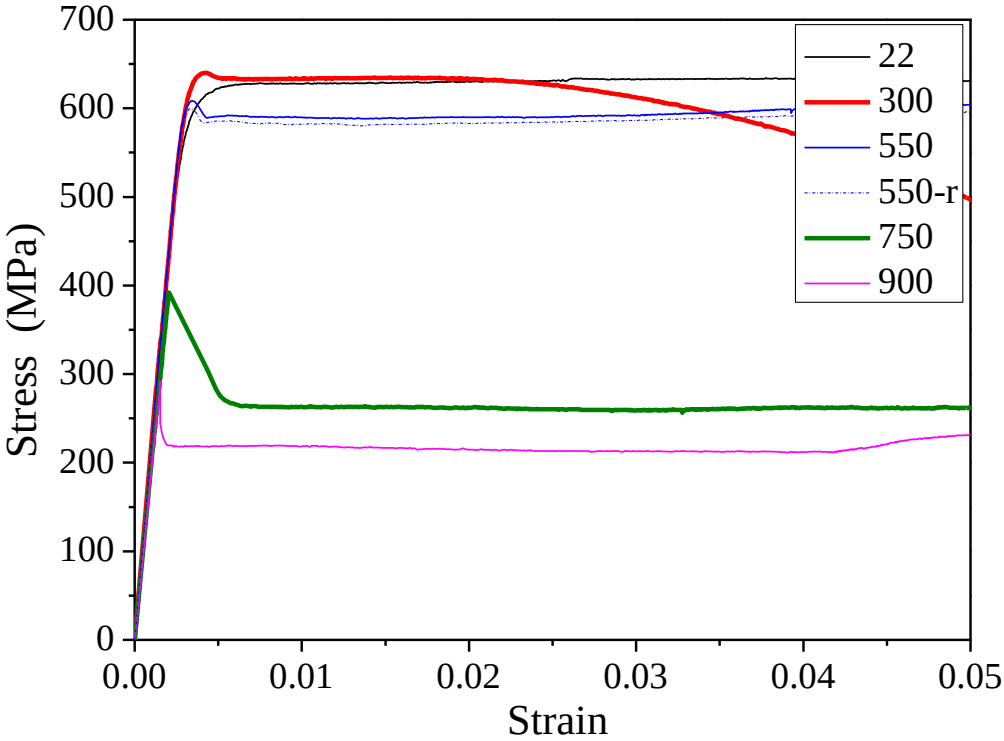

b) Initial parts of complete curves

Figure 11: Stress-stain curves of Series 120-G500 by electric furnace

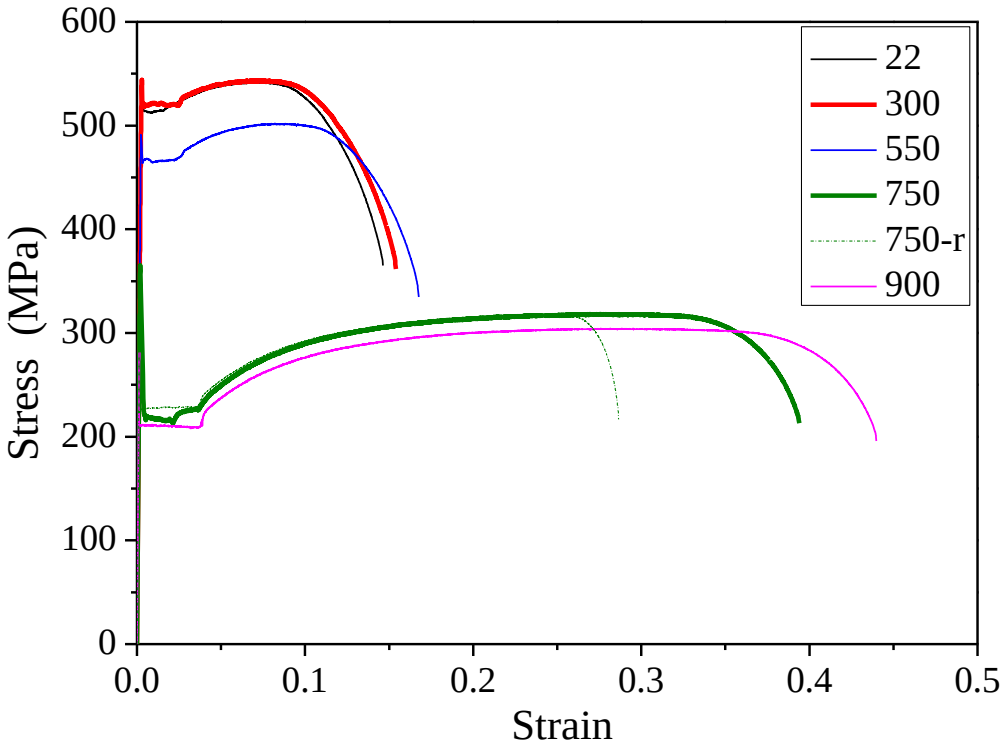

a) Complete curves

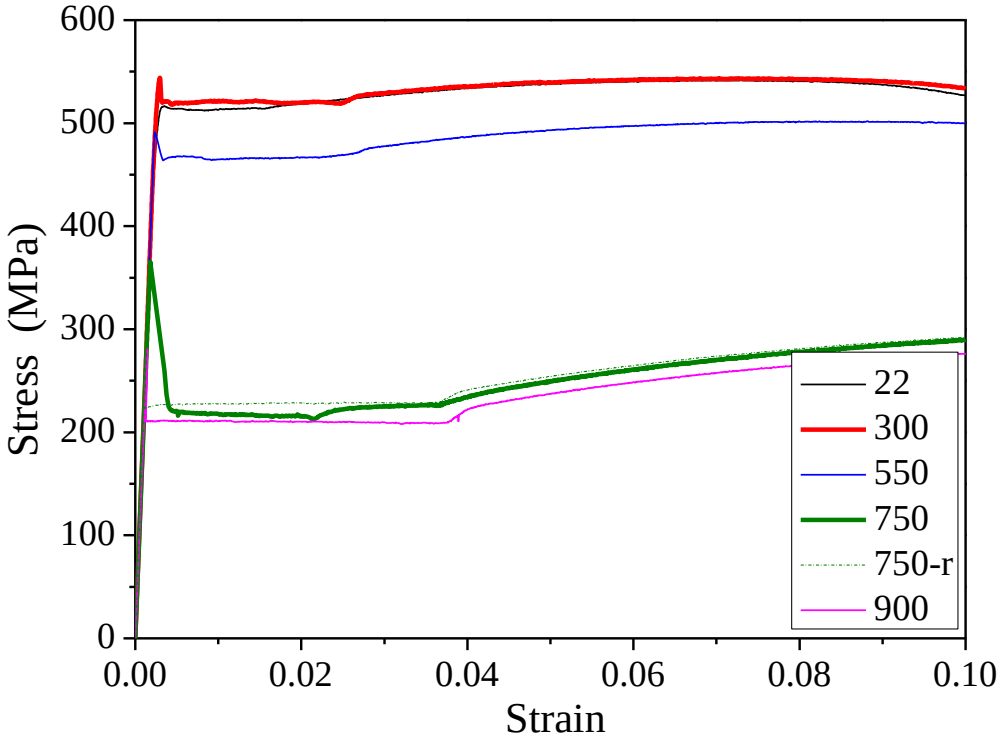

b) Initial parts of complete curves

Figure 12: Stress-stain curves of Series 190-G450 by electric furnace

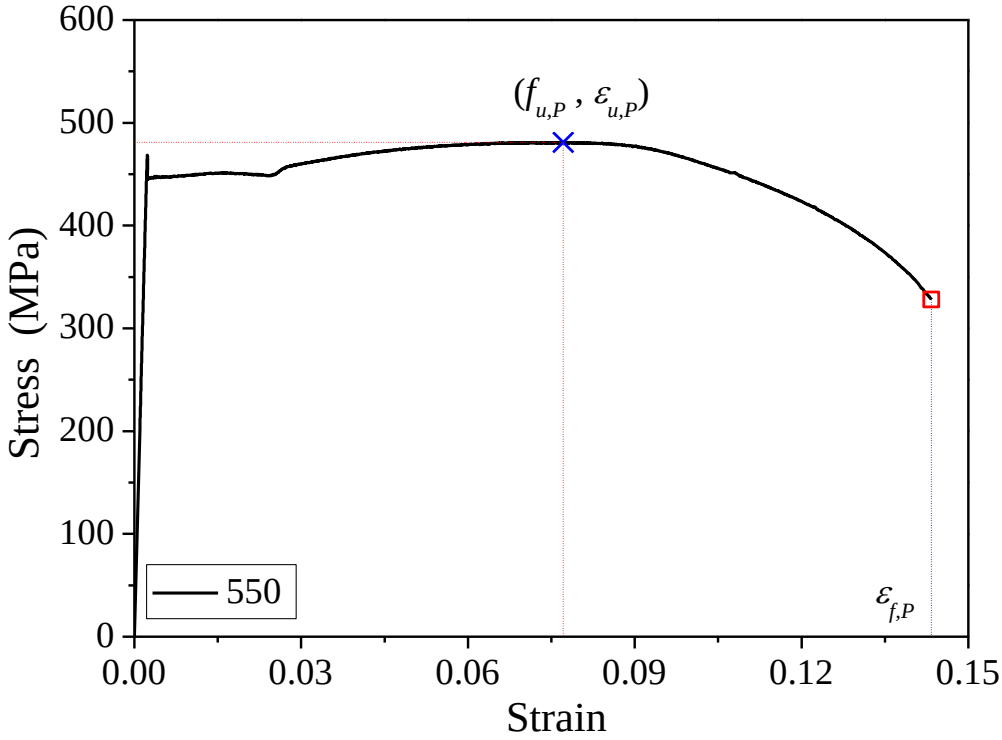

a) Complete stress-strain curve

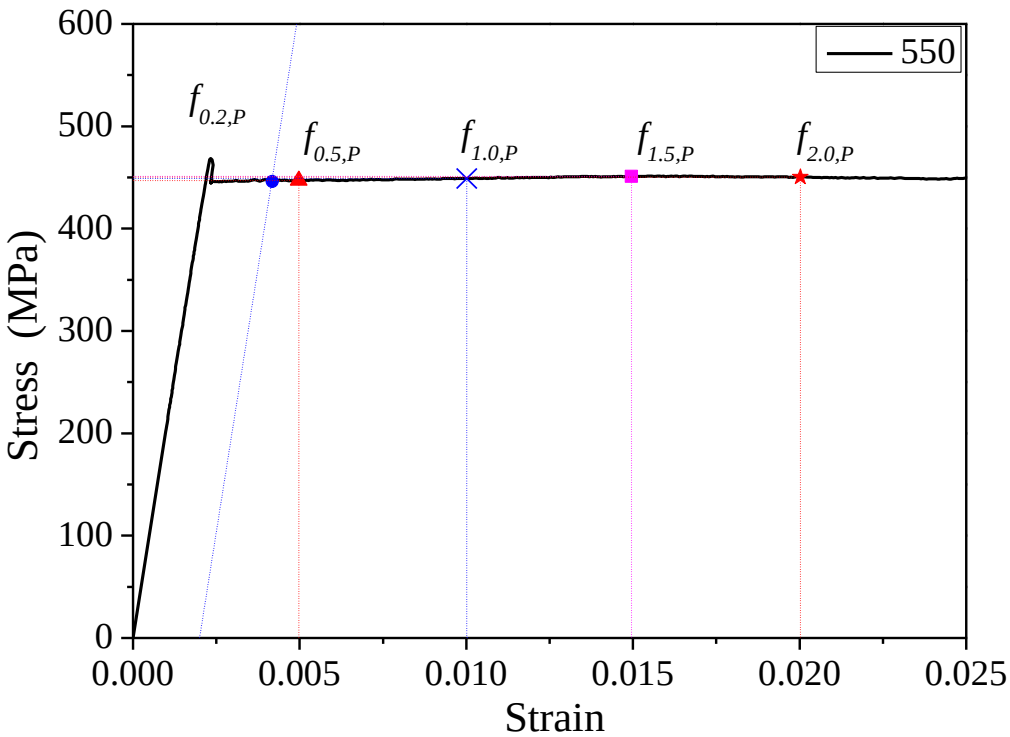

b) Initial part of complete stress-strain curve

Figure 13: Definition of symbols in material properties (e.g, Specimen 190-G450 by LPG furnace)

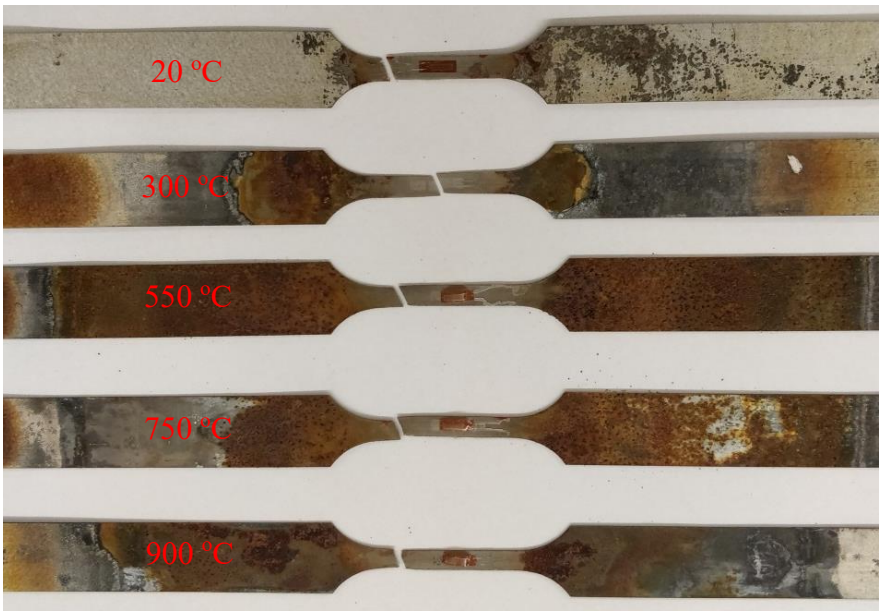

a) Specimens Series 042-G550 by electric furnace

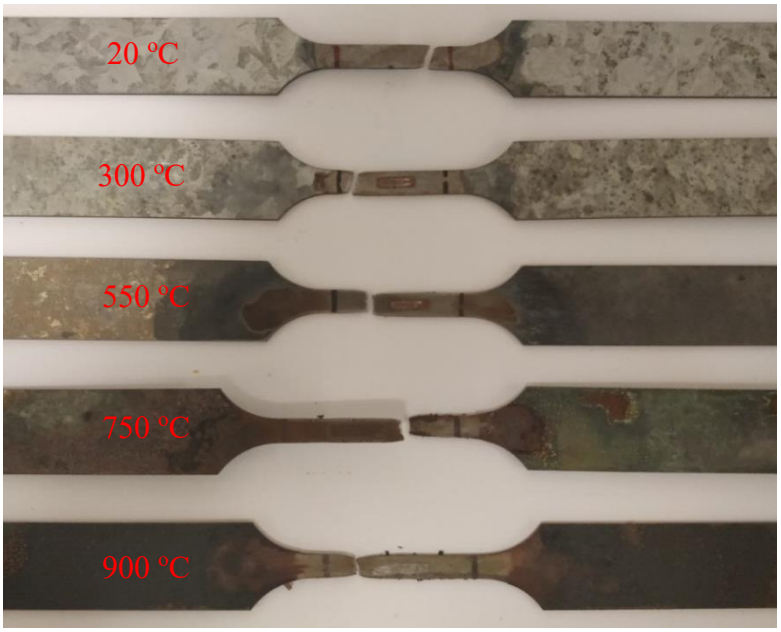

b) Specimens Series 120-G500 by LPG furnace

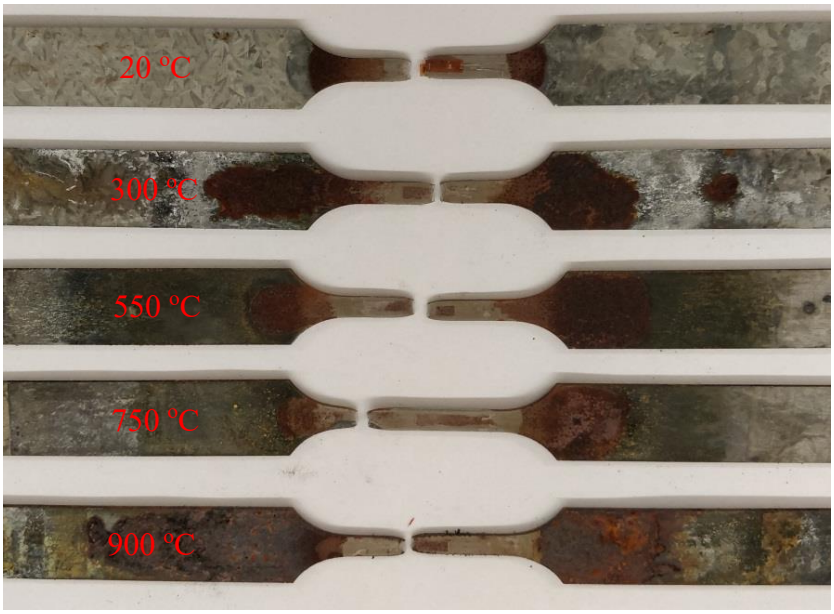

c) Specimens Series 190-G450 by electric furnace

Figure 14: Failure mode of TSS coupon specimens after exposure to high temperatures

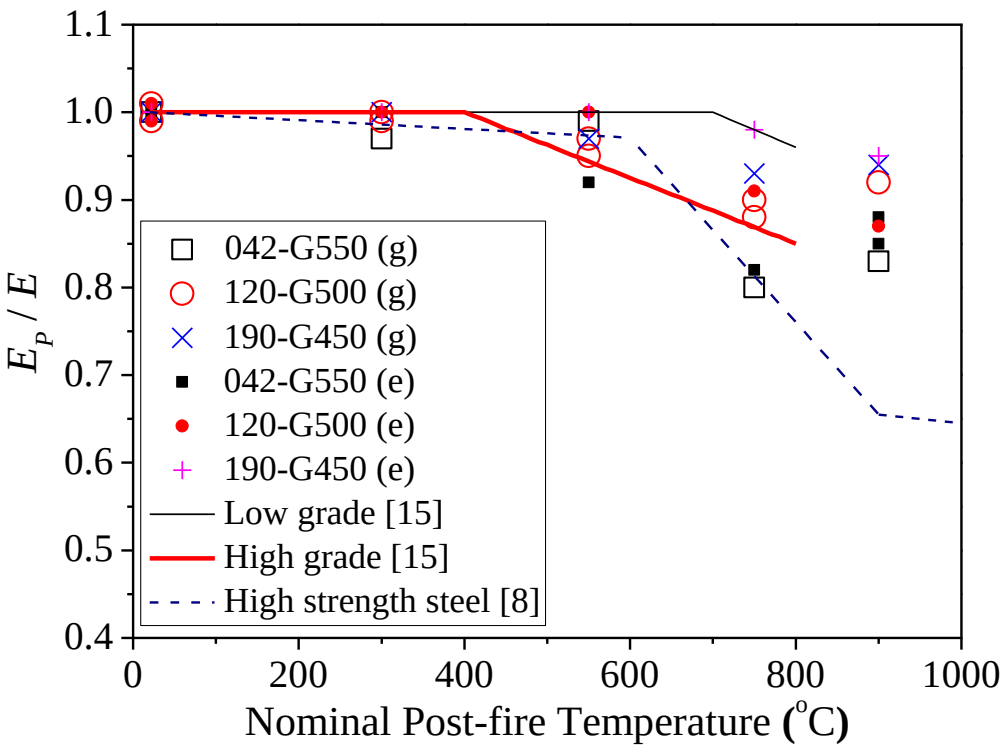

Figure 15: Comparison of retention factors for Young's Modulus

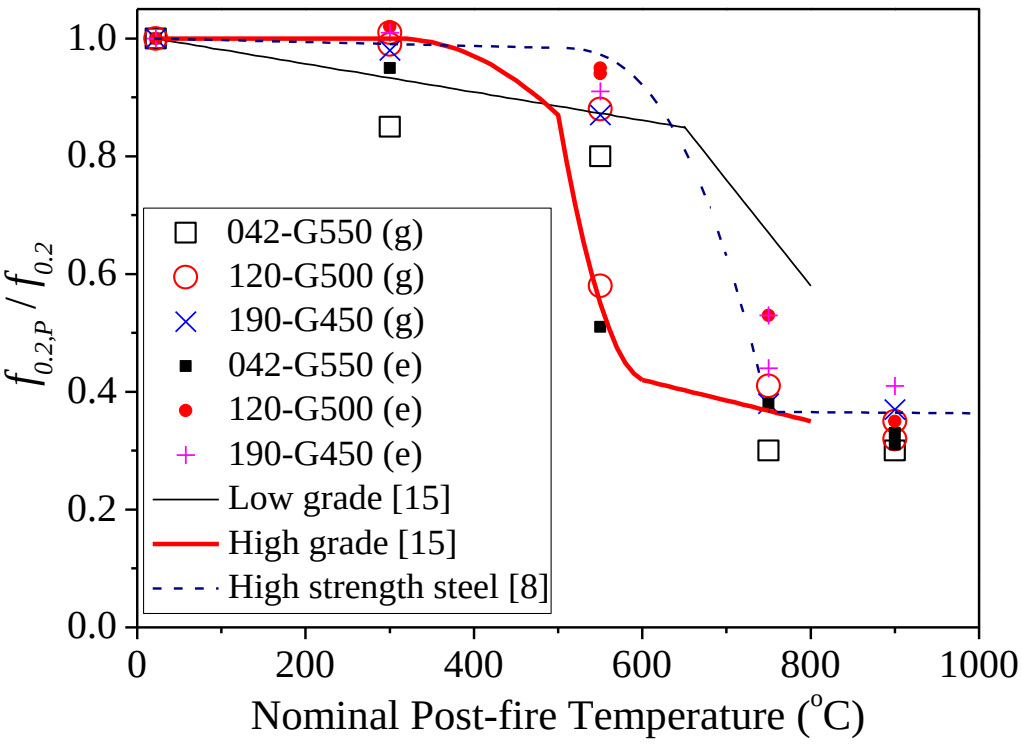

Figure 16: Comparison of retention factors for 0.2% proof stress

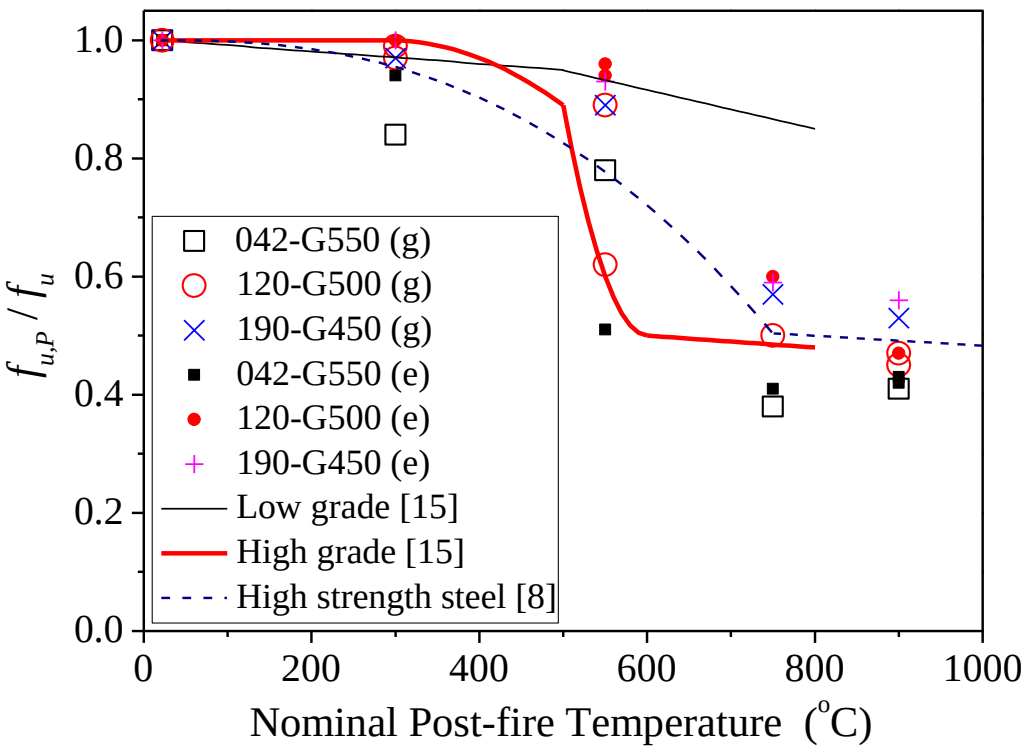

Figure 17: Comparison of retention factors for ultimate strength

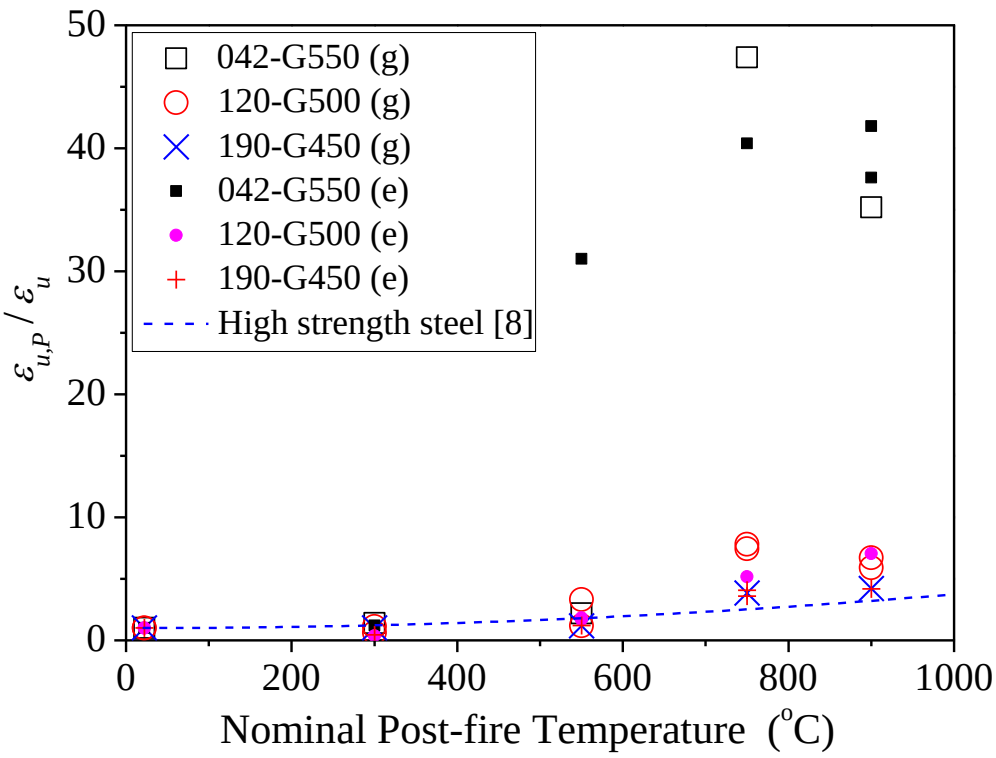

Figure 18: Comparison of retention factors for ultimate strain

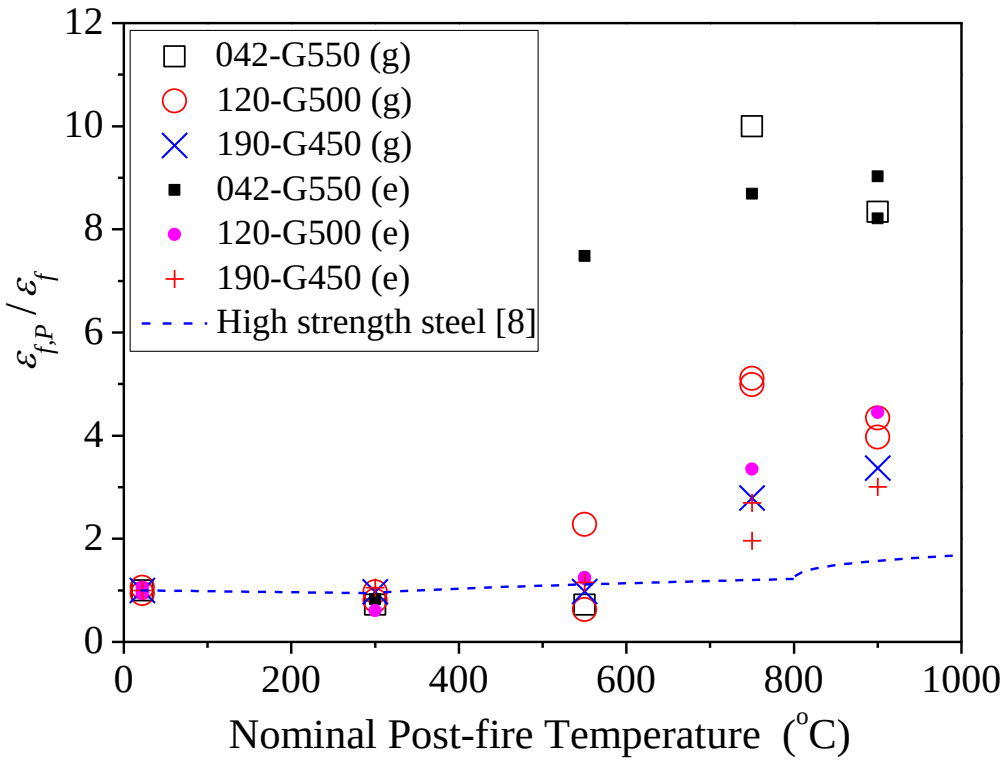

Figure 19: Comparison of retention factors for fracture strain

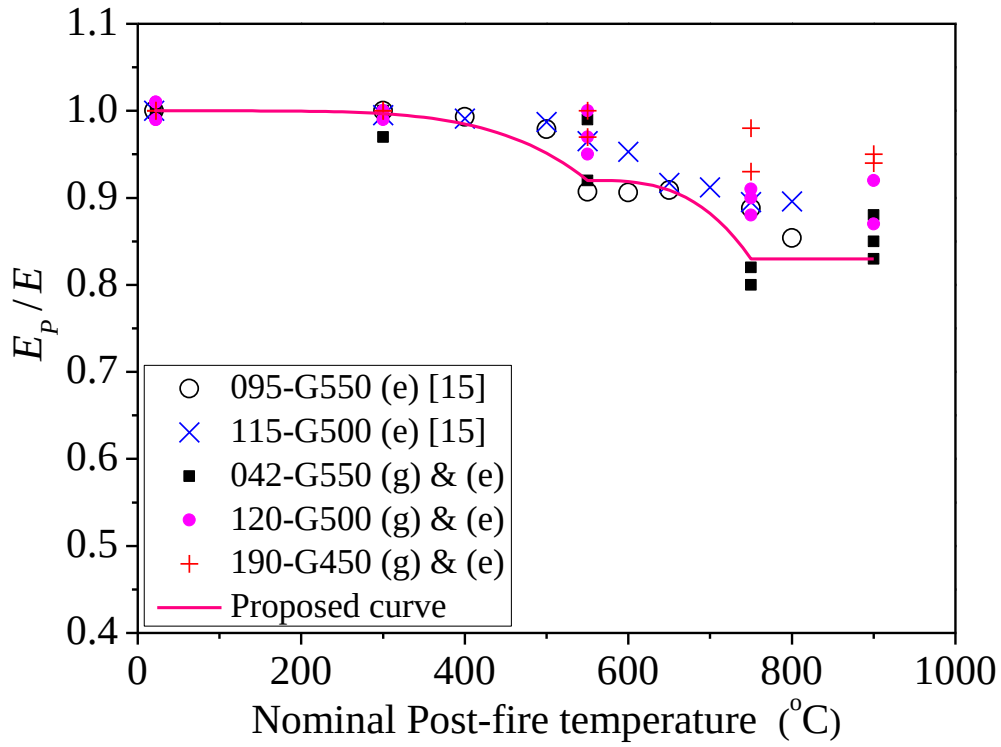

Figure 20: Proposed curves for retention factor of Young's Modulus

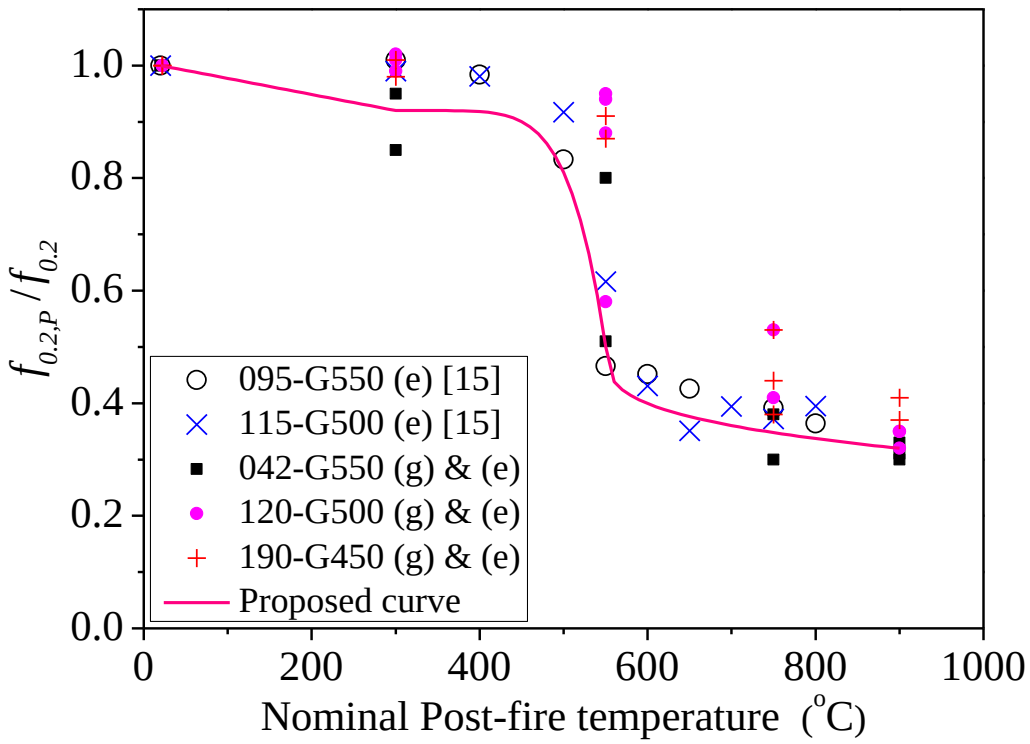

Figure 21: Proposed curves for retention factor of 0.2% proof stress

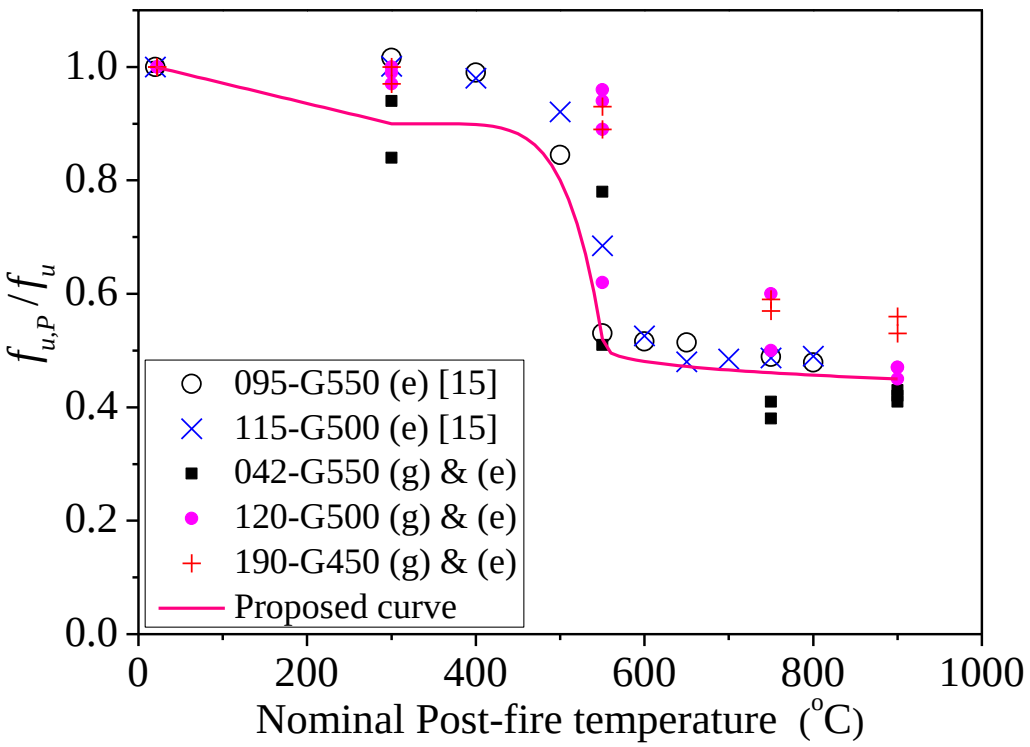

Figure 22: Proposed curves for retention factors of ultimate strength

Table 1: Mechanical properties of TSS without exposed to high temperature

Specimen	E (GPa)	$f_{0.2}$ (MPa)	$f_{0.5}$ (MPa)	$f_{1.0}$ (MPa)	$f_{1.5}$ (MPa)	$f_{2.0}$ (MPa)	f_u (Mpa)	ε_u (%)	ε_f (%)
042-G550	228	775	788	755	756	745	788	0.5	2.9
120-G500	218	622	622	628	629	630	634	3.8	8.4
120-G500-r	221	622	623	628	629	630	635	3.9	9.5
190-G450	212	513	514	513	515	519	542	6.6	14.6

Note: “r” means repeated test.

Table 2: Mechanical properties of TSS after exposure to high temperatures in LPG furnace

Series	T (°C)	T_m (°C)	E_P (GPa)	$f_{0.2,P}$ (MPa)	$f_{0.5,P}$ (MPa)	$f_{1.0,P}$ (MPa)	$f_{1.5,P}$ (MPa)	$f_{2.0,P}$ (MPa)	$f_{u,P}$ (Mpa)	$\varepsilon_{u,P}$ (%)	$\varepsilon_{f,P}$ (%)
042-G550	300	284.2~338.8	221	655	678	655	638	598	658 (702)#	0.7 (0.4)#	2.1
	550	517.2~578.9	225	619	618	613	600	514	615 (658)#	1.1 (0.3)#	2.1
	750	746.4~769.3	182	230	230	233	232	235	301	23.7	29.0
	900	895.2~918.0	189	231	232	234	237	239	322	17.6	>24.2
120-G500	300	284.2~338.8	218	614	615	611	613	611	614 (620)#	4.3 (0.4)#	8.7
	300	284.2~338.8	220	628	629	625	625	625	627 (632)#	2.4 (0.4)#	7.2
	550	517.2~578.9	212	547	546	552	556	558	564	4.5	5.6
	550	517.2~578.9	208	358	357	355	355	356	396	12.8	20.4
	750	746.4~769.3	197	257	258	259	260	261	319	28.6	45.7
	750	746.4~769.3	193	257	256	258	260	261	315	30.1	44.7
	900	895.2~918.0	202	215	215	216	217	218	301 (315)#	22.7 (0.2)#	35.5
	900	895.2~918.0	193	200	200	199	200	199	285 (279)#	25.8 (0.2)#	38.7
190-G450	300	284.2~338.8	209	503	505	505	506	504	528 (529)#	6.6 (0.3)#	14.2
	550	517.2~578.9	206	446	447	449	451	450	481	7.7	14.3
	750	746.4~769.3	197	195	207	223	217	215	307	25.5	40.8
	900	895.2~918.0	200	189	190	192	194	194	288	27.8	49.2

Note: (x)# result at the first peak in the stress-strain curve.

Table 3 Mechanical properties of TSS after exposure to high temperatures in electrical furnace

Series	T (°C)	T_m (°C)	E_P (GPa)	$f_{0.2,P}$ (MPa)	$f_{0.5,P}$ (MPa)	$f_{1.0,P}$ (MPa)	$f_{1.5,P}$ (MPa)	$f_{2.0,P}$ (MPa)	$f_{u,P}$ (Mpa)	$\varepsilon_{u,P}$ (%)	$\varepsilon_{f,P}$ (%)
042-G550	300	293.8~300.4	229	736	752	736	723	679	740 (775)#	0.6 (0.4)#	2.4
	550	551.5~555.3	210	392	389	388	383	377	405 (429)#	15.5 (0.2)#	21.7
	750	752.1~759.5	188	293	282	278	278	274	326 (350)#	20.2 (0.2)#	25.2
	900	886.7~901.8	193	255	253	247	247	245	341	18.8	26.2
	900	886.7~901.8	201	242	243	253	260	266	333	20.9	23.8
120-G500	300	293.8~300.4	219	633	634	633	634	633	635 (640)#	1.4 (0.4)#	5.5
	550	551.5~555.3	220	591	591	590	589	590	608 (608)#	7.0 (0.3)#	11.2
	550	551.5~555.3	219	587	585	582	582	583	599 (600)#	6.5 (0.3)#	11.0
	750	752.1~759.5	199	329	279	263	263	262	382 (392)#	19.9 (0.2)#	30.0
	900	886.7~901.8	191	218	218	218	217	215	298	27.1	39.8
190-G450	300	293.8~300.4	213	516	520	521	521	520	544	3.0	15.4
	550	551.5~555.3	213	468	468	465	466	467	502	8.0	16.8
	750	752.1~759.5	207	271	220	218	216	216	318 (365)#	26.8 (0.2)#	39.4
	750	752.1~759.5	208	225	227	228	228	228	318 (331)#	23.7 (0.2)#	28.6
	900	886.7~901.8	201	208	211	211	210	210	304	27.6	44.0

Note: (x)# result at the first peak in the stress-strain curve.

Table 4 Number of data used for proposed retention factors after exposure to high temperatures

Steel grade	Nominal thickness (mm)	$f_{0.2}$ (MPa) Nominal	$f_{0.2}$ (MPa) Measured	E_P/E	$f_{0.2,P}/f_{0.2}$	$f_{u,P}/f_u$
G450	1.90	450	775	10	10	10
G500	1.20	500	622	15	15	15
G550	0.42	550	513	10	10	10
G500 [15]	1.15	500	664	10	10	10
G550 [15]	0.95	550	664	9	9	9
Total number of data				54	54	54

Table 5 Coefficients retention factors of TSS after exposure high temperatures

Retention factor	Proposed coefficients				
	T (°C)	a	b	c	n
k_E ($k_E = E_P/E$)	$20 < T \leq 550$	1.00	20	5.227×10^{14}	5
	$550 < T \leq 750$	0.92	550	8.889×10^{7}	3
	$750 < T \leq 900$	0.83	-	-	-
$k_{0.2}$ ($k_{0.2} = f_{0.2,P}/f_{0.2}$)	$20 < T \leq 300$	1.00	20	3.500×10^{3}	1
	$300 < T \leq 550$	0.92	300	5.813×10^{14}	6
	$550 < T \leq 900$	0.50	550	3.220×10	0.3
k_u ($k_u = f_{u,P}/f_u$)	$20 < T \leq 300$	1.00	20	2.800×10^{3}	1
	$300 < T \leq 550$	0.90	300	6.425×10^{14}	6
	$550 < T \leq 900$	0.52	550	8.280×10	0.3